# Hofbauer cells in pregnancies complicated by gestational diabetes mellitus and pathological fetal growth.

Georgia Fakonti[1], Georgia Mappa[2], Nicolas Orsi[2], Eleanor M. Scott[1], Beth Holder[3*], Karen Forbes[1*]

[1]Leeds Institute of Cardiovascular and Metabolic Medicine, University of Leeds, Leeds, United Kingdom

[2]Leeds Institute of Medical Research at St James's, University of Leeds, Leeds, United Kingdom

[3]Institute of Reproductive Biology, Imperial College London, London, United Kingdom

*corresponding authors

## Abstract

**Problem:** Gestational diabetes mellitus (GDM) increases the risk of large-for-gestational-age (LGA) birth and long-term cardiometabolic complications in offspring, particularly in males. These outcomes are associated with altered placental vascularisation, but the underlying mechanisms remain poorly defined. Hofbauer cells (HBCs) are fetal-origin macrophages located in the villous stroma with established roles in immune regulation and vascularisation.

**Method of Study:** This study investigated whether HBC abundance and phenotype are associated with fetal growth, fetal sex and placental vascularisation in term placentae from non-GDM and GDM pregnancies. Pan-macrophage (CD14, CD68), HBC-enriched (FOLR2,VSIG4), M1 (CD86), and M2 (CD163, MRC1) markers were assessed by RT-qPCR and quantitative immunohistochemistry.

**Results:** In both non-GDM and GDM placentae, all markers, except CD86 were detected, supporting an M2-like HBC phenotype. In GDM placentae, the number of pan-macrophage (CD68), HBC-enriched (FOLR2), and M2-associated (CD163, MRC1) cells were reduced in terminal villi compared with non-GDM controls ($p<0.05$; n=9 non-GDM; n=9 GDM), indicating reduced HBC abundance without phenotypic switching. Reduced expression of HBC-enriched (FOLR2, VSIG4) and M2-associated (CD163) transcripts supported these findings($p<0.05$; n=18 non-GDM and n=19 GDM). No further differences were observed following stratification by fetal growth or sex. HBC-related gene expression correlated positively with the endothelial marker PECAM1/CD31, in both non-GDM and GDM placentae ($r \geq 0.5$, $p<0.05$)

**Conclusions:** HBCs abundance is reduced in GDM placentae independently of fetal growth or sex, whilst HBC phenotype is preserved. Reduced HBC abundance may contribute to placental vascular alterations that are characteristic of GDM.

**Keywords**: Gestational diabetes mellitus, GDM, placenta, macrophages, Hofbauer cells, LGA

## 1. Introduction

Diabetes in pregnancy is considered a high-risk condition for both mother and offspring. Pregnant women with diabetes, either pre-existing or arising during pregnancy, known as gestational diabetes mellitus (GDM), have an increased risk of pregnancy complications. These include complications related to birth outcome (stillbirth, miscarriage, preterm birth) and offspring health (later development of obesity, diabetes, and cardiovascular diseases) (Clement et al., 2024; Ye et al., 2022). Diabetes in pregnancy is also associated with impaired fetal cardiac function and

structure, suggesting that cardiovascular diseases may be initiated at early stages of fetal development (Depla et al., 2021; Mahadevan et al., 2023). Babies born to mothers with diabetes have high risk of pathological fetal growth and are often large for gestational age (LGA; >90th centile), rather than appropriate for gestational age (AGA) (Bommarito et al., 2023; Murray and Reynolds, 2020). This can lead to several early-life and long-term complications, such as obesity and metabolic conditions, with male offspring at particularly high risk (Li et al., 2017; Nielsen et al., 2012). Despite these well-established clinical associations, the placental immune mechanisms linking maternal diabetes to abnormal fetal growth and adverse pregnancy outcomes remain poorly defined.

Several theories on the origin of fetal growth complications in diabetes have been proposed, including the impact of maternal hyperglycaemia and fetal hyperinsulinemia (Leach et al., 2009), with even subtle glucose changes during pregnancy reported to impact growth (Law et al., 2015; Scott et al., 2022). However, the placental molecular and cellular mechanisms that drive the increased risk of pregnancy complications and LGA offspring remain largely unknown. Research increasingly supports the Developmental Origins of Health and Disease (DOHaD) hypothesis, suggesting that adult disease risk may be programmed during early development (Lacagnina, 2019). Adverse *in utero* conditions can shape fetal development through long-lasting programming effects, including on immune development and function (Chen et al., 2016). This positions pregnancy as a critical window during which placental dysfunction may influence both short-and long-term outcomes.

Situated at the interface between the maternal and fetal circulations, the placenta is highly sensitive to changes in the maternal environment. Within the placental villous tree, terminal villi are the primary site of maternal-fetal exchange (Erlich et al., 2019),

due to their minimal diffusion distance between maternal and fetal blood. This close proximity may render terminal villi particularly vulnerable to metabolic and inflammatory alterations associated with GDM (Byford et al., 2021; Owen et al., 2024). Indeed, GDM placentae exhibit alterations in placental inflammatory mediators, villous maturity, placental vasculature (such as reduced branching and increased capillary density), and extracellular matrix (Kang et al., 2022; Lu et al., 2022; Radaelli et al., 2003). However, the mechanisms driving these changes and their relation to fetal growth in GDM remain elusive.

Hofbauer cells (HBCs)- fetal-origin macrophages, are abundant within terminal villi and are well placed to mediate alterations associated with pathological fetal growth. HBCs play established roles in immune regulation (Fakonti et al., 2022), tissue growth, and remodelling (Reyes and Golos, 2018; Seval et al., 2007), and interact closely with mesenchymal and endothelial cells to influence villous development (Ingman et al., 2010). Given their involvement in inflammation and remodelling, alterations in HBC abundance or phenotype could plausibly contribute to placental dysfunction and abnormal fetal growth in GDM. GDM is characterised by a chronic low-grade inflammatory state, which may exacerbate placental metabolic and vascular dysfunction (Di Simone et al., 2008, 2006; Mallardo et al., 2021). However, HBC abundance and phenotype in terminal villi and their potential role in pathological fetal growth in GDM remain poorly defined.

Macrophages are often categorised into classically-activated (M1; pro-inflammatory) and alternatively-activated (M2; anti-inflammatory/tissue-remodelling) phenotypes. Their polarisation from M0 depends on environmental signals that induce expression of different markers (e.g. M1:CD80, CD86 and M2: MRC1, CD163) and secretion of distinct cytokines. Although, this classification is oversimplified and there are many

subtypes beyond the M1/M2 dichotomy, HBCs seem to maintain an anti-inflammatory/tissue remodelling phenotype even in the presence of infection and are considered to maintain a M2 phenotype in diabetes (Fakonti et al., 2022; Schliefsteiner et al., 2017). In this study we quantified the abundance of HBCs in terminal villi and assessed the expression of pan-macrophage (CD14, CD68), HBC-enriched (FOLR2 and VSIG4) (Thomas et al., 2020), M1 (CD86), and M2 (CD163 and MRC1) markers placentas from non-GDM and GDM pregnancies with AGA or LGA infants. We further examined whether HBC abundance or phenotype was associated with fetal sex or markers of villous vascularisation.

## 2. Materials and methods

### 2.1 Patient groups

All research was conducted following ethical approval from North West Regional Ethics Committee (08/H1010/55+5) and London Riverside Research Ethics Committee under the REC reference number 18/LO/0067 and IRAS project ID 234385. Pregnant women were recruited following written informed consent at Leeds Teaching Hospitals Trust or Manchester University NHS Foundation Trust. Placentae from term (≥37 weeks of gestation, live births) singleton uncomplicated pregnancies and pregnancies complicated by GDM with and without pathological fetal growth were studied. GDM was diagnosed by routine oral glucose tolerance test and fetal growth was calculated by estimating the fetal percentile using the World Health Organization growth calculator (“Fetal Growth Calculator,” n.d.; Kiserud et al., 2018). Babies born ≥ 90th centile were classified as LGA, and all >10th and <90th centile were classified as AGA. The human tissue processing, data curation and analysis were conducted in accordance with Declaration of Helsinki guidelines, General Data Protection

Regulation, and Human Tissue Act. Two independent patient cohorts were utilised for RT-qPCR and immunohistochemistry studies.

### 2.2 Tissue processing

Placental tissue was collected within 30-60 minutes of delivery. Fetal membranes and cord were removed, and the trimmed placenta was weighed. Three full thickness portions, approximately 2cm$^3$, were taken at random from the centre, edge and middle regions of the placenta and washed in phosphate buffered saline (PBS). For immunohistochemistry experiments, a full-thickness sample (~1cm$^3$) was dissected, washed in PBS, fixed in 10% neutral buffered formalin (HT501128, Sigma-Aldrich), and embedded in paraffin. For RNA analyses, the chorionic and basal plate were removed before each portion was dissected further into ~0.25cm$^3$ pieces which were refrigerated in RNAlater® overnight, snap frozen, and transferred to -80°C for future RNA extraction.

### 2.3 Immunohistochemistry

Tissue sections (5μm) were mounted on poly-l-lysine coated slides and then heated to 60°C for 20min, followed by incubation in HistoClear (NAT1330D2, SLS) for deparaffinization, and rehydration by passing through graded ethanol baths. Heat-induced antigen retrieval was performed using sodium citrate (0.01M, pH 6.0, 2x5min) followed by quenching endogenous peroxidase activity by incubating for 15min with 3% hydrogen peroxide. Slides were washed with Tris Buffered Saline (TBS) (0.02M Trisma Base, 0.15M NaCl, pH=7.4, 2x5min) and blocked with bovine serum albumin (5% in TBS) for 1h. Sections were incubated overnight at 4°C with primary antibody or IgG control (**Table 1**), then washed and incubated with biotinylated secondary

antibody for 1h at room temperature (**Table 1**). After further TBS washes, avidin peroxidase was applied (A3151, Sigma-Aldrich) (0.02μM in high salt TBS; 0.005M Trisma Base, 0.3M NaCl) for 30min. ImmPACT DB EqV substrate kit, peroxidase (SK-4103, Vector lab) used for detection with haematoxylin (1092530500, Merck) counterstaining. Slides were dehydrated, cleared in HistoClear and mounted in DPX (Thermo Fisher Scientific). To was confirm that the absence of staining (CD86) in placental tissue was due to antigen absence and not procedure, positive controls (human myometrium) were used.

Microphotographs obtained using Zeiss Axioscan Z1 slide scanner (20x magnification). Analysis was performed semi-automated and blinded to any clinical data in QuPath (Bankhead et al., 2017). Colour deconvolution was applied to obtain single stained-haematoxylin only images to minimise the risk of selection bias. Terminal villi (17/image) were selected based on consistent morphological criteria, such as the size as they are typically smaller than intermediate and stem villi with numerus capillaries and minimal dilation distance from the syncytiotrophoblast layer, with similar total area between groups (**Supplementary Figure 1-4**). A border was manually drawn around each villi, cells within the villus stroma, but outside of the fetal vessels were counted, and data were normalised to villous area ($mm^2$) using standardised QuPath pipelines (Bankhead et al., 2017).

### 2.4 RNA extraction, cDNA synthesis, and quantitative reverse transcription PCR (RT-qPCR)

Total RNA was extracted from 0.25g of placenta tissue using the mirVana™ miRNA isolation kit (AM1561, Thermo Fisher Scientific) according to the manufacturer's guidelines for frozen tissue and purified with the RNA clean and concentrator-5 kit

(R1013, Zymo Research), including DNase I treatment before RNA clean-up according to manufacturer's instructions. The concentration and quality of the eluted RNA was measured with a NanoDrop ND-1000 Spectrophotometer. RNA (100ng) was converted to cDNA using the AffinityScript cDNA Synthesis Kit (200436, Agilent) following the manufacturer's instructions. Controls with no reverse transcriptase and no template were also prepared. RT-qPCR was performed using qPCR Brilliant III SYBR MM with ROX kit (600882, Agilent) and gene specific primers (Integrated DNA Technologies) (**Table 2**) following the manufacturer's instructions using LightCycler96 (Roche) with the following parameters: 1 cycle (3min/95°C), 40 cycles (20 sec/95°C, 20sec/primer-specific annealing temperature). A melting curve was included by incubating the samples at 95°C for 1min, followed by incubation at 55 °C for 30 sec. The temperature was then increased to 95°C, ramping at 0.2°C/cycle. For each plate, an interplate calibrator sample was included. All samples were run in duplicates (Ct difference between duplicates <0.5) and the $\Delta\Delta C_t$ method was used to analyse the data.

### 2.5 Statistical analysis

Data distribution was assessed using the Shapiro-Wilk test. Continuous variables with normal distribution are shown as mean ± standard deviation (SD) and analysed by unpaired t-test (two-tailed) or one-way ANOVA followed by Tukey's post-hoc test (equal SD) or Brown-Forsythe and Welch ANOVA followed by Dunnett T3 post-hoc test (non-equal SD). Continuous variables that were not normally distributed are presented as median (q1, q3) and were assessed using Mann-Whitney (two-tailed) or Kruskal–Wallis with Dunn's post-hoc test. Categorical variables are presented as absolute and relative frequencies (%) and analysed by Fisher-exact or Chi-squared

tests. The interaction between diabetes and fetal growth, or fetal sex was assessed by two-way ANOVA. When data was not normally distributed, data were transformed using natural logarithm (ln). Data was considered statistically significant when $p<0.05$. Analysis was performed using GraphPad (v.10.3.1) and correlation matrix was created using the corrplot package in R (v.4.3.1).

## 3. Results

### 3.1 Expression levels and phenotype of HBCs in GDM placentae

GDM and non-GDM participants were comparable with respect to maternal age, parity, smoking status, booking BMI, fetal sex and gestational age at delivery for both RT-qPCR and immunohistochemistry analyses (**Table 3**). Pan macrophage (M0; CD68), M2-associated (MRC1, CD163) and HBC-enriched (FOLR2) markers were detected at both the transcript (**Figure 1A-C**) and protein (**Figure 2A-D**) levels in placental villous tissue from both non-GDM and GDM pregnancies. The M1-associated marker CD86, was undetectable in human placental tissue in either group (**Figure 2E**) despite robust expression in human uterine tissue used as a positive control (**Figure 2F**).

At the transcript level, no differences were detected in the pan-macrophage markers CD14 ($p=0.77$) or CD68 ($p=0.10$) expression between groups (**Figure 1A**). In contrast, IHC revealed a significant reduction in the number of CD68 +ve cells, per villous area ($mm^2$) in GDM placentae compared with non-GDM (non-GDM: 522 ± 178, GDM: 337 ± 119; $p<0.01$) (**Figure 2A**).

Expression of the HBC-enriched markers FOLR2 and VSIG4 was reduced at the mRNA levels in GDM placentae (both $p=0.03$; **Figure 1C**), accompanied by fewer HBCs (FOLR2+ cells) per villous area (non-GDM: 1223±5883 cells/$mm^2$; GDM: 750±427 cells/$mm^{2;}$ $p=0.03$; **Figure 2D**). Similarly, CD163 mRNA expression was

lower in GDM placentas (p=0.01; **Figure 1B**), with a corresponding reduction in the number of CD163+ cells (non-GDM: 1122 ± 268 cells/mm$^2$; GDM: 857 ± 291 cells/mm$^2$; p=0.03; **Figure 2B**). Although MRC1 transcript levels was not different between groups (**Figure 1B**), the number of MRC1+ cells was significantly reduced in GDM placentae (non-GDM: 881±267 cells/mm$^2$; GDM: 430±242 cells/mm$^2$; p<0.001; **Figure 2C**), potentially suggesting alterations in post transcriptional control of MRC1.

### 3.2 Effect of GDM and pathological fetal growth on HBC number and phenotype

To determine whether changes in HBC abundance or phenotype were associated with pathological fetal growth, samples were stratified based by birthweight category (AGA compared to LGAl **Supplementary Table 1-2**). No differences in pan-macrophage, HBC-enriched, M1 or M2 -associated markers were observed between AGA and LGA groups in either non-GDM or GDM placentae (**Figure 3**).

### 3.3 Fetal sex differences in HBC number and phenotype

Given reported sex differences in perinatal outcomes (Hu et al., 2020; Retnakaran and Shah, 2015) and placental immune responses (Pantazi et al., 2022), data were stratified by fetal-sex (**Supplementary Tables 3 & 4).** No sex-specific differences were detected in transcript or abundance of pan-macrophage- or HBC-enriched markers in non-GDM or GDM placentae (**Figure 3A &B**), indicating that the observed alterations associated with GDM were not sex-dependent.

### 3.4 Correlation of HBCs and placental vascular markers

HBCs exhibit an M2 phenotype, and display close proximity to placental vasculature (**Figure 4A**). As PECAM1/CD31 expression was previously shown to be reduced in GDM compared to non-GDM placentae (Byford et al., 2025), we assessed associations between PECAM1 mRNA expression and HBC-related markers (**Figure 4B-C**). In non-GDM placentae, PECAM1 expression correlated positively with CD163 ($r=0.62$; $p\leq0.01$), VSIG4 ($r=0.61$; $p\leq0.01$) and FOLR2 ($r=0.58$; $p<0.05$) (**Figure 4B**). Similar associations were observed in GDM placentae for PECAM1 with FOLR2; ($r=0.51$; $p<0.05$) and CD163 ($r=0.57$; $p<0.05$) (**Figure 4C**). Correlation matrices further revealed strong positive relationships between macrophage- and HBC-enriched markers in both non-GDM ($r\geq5$, $r\leq0.86$, $p<0.05$) and GDM placentae ($r\geq0.75$, $r\leq0.89$; $p\leq0.001$) (**Figure 4B-C**).

## 4. Discussion

This study investigated HBC numbers and phenotype in term placentae from non-GDM and GDM pregnancies, exploring their associations with LGA, fetal sex, and placental vascularisation. We demonstrate that HBC, abundance but not phenotype, is reduced in term placentae from pregnancies complicated by GDM. The consistency of our findings at both the transcript and protein level across two independent cohorts strengthens confidence that GDM alters fetal macrophage presence within the villous tree. Importantly, these changes were independent of fetal growth status or fetal sex, indicating that reduced HBC abundance is a fundamental placental consequence of GDM rather than an adaptive response to fetal overgrowth, and is unlikely to contribute to LGA development.

The observed decrease in the number of HBCs in terminal villi of GDM placentae aligns with a previous studies showing a reduction in FOLR2 gene expression in GDM placental lysates (Alur et al., 2021), although it contrasts with other studies showing increased gene expression of macrophage genes and a higher number of HBCs in placentae from GDM placentae (Dairi et al., 2020; Kerby et al., 2021; Mrizak et al., 2014; Yu et al., 2013). These discrepancies could arise from variations in demographic characteristics among participants (Koru-Sengul et al., 2016; Nandy et al., 2011), however, it is more likely that they arise from methodological differences. Earlier studies quantified HBCs across whole sections without controlling for villous subtype or villous area or villous type-factors that can strongly influence cell density. We focused on terminal villi as they are more likely to be highly influenced by components of the maternal circulation. By restricting our analysis to morphologically matched terminal villi and normalising to villous area, we minimised sampling bias and obtained a more accurate and anatomically meaningful measure of HBC abundance. This methodological clarity likely explains the more coherent patterns observed across our datasets. The overall reduction in HBC-enriched gene expression and HBC number suggests a disruption in fetal macrophage presence that could influence villous immune homeostasis.

Consistent with previous literature, our study found no evidence of M1 polarisation. M1 markers were undetectable in the placenta villous tree, whereas M2 macrophage markers were consistently detected at both mRNA and protein level, supporting the concept that HBCs exhibit an M2 anti-inflammatory, tissue-remodelling phenotype even in the context of metabolic stress (Schliefsteiner et al., 2017; Zhang et al., 2022). The preserved M2-like phenotype may reflect intrinsic fetal programming to protect the developing fetus from an excessive inflammatory environment that is potentially

mediated by epigenetic regulation of M1 and M2 genes (Kim et al., 2012). It is likely that a reduction in HBCs is associated with functional impacts in GDM placentae that are associated with M2 phenotype macrophages. Although we investigated HBCs in third trimester, their roles in early pregnancy may be distinct (Yoshida et al., 2025) and potentially pivotal in influencing the placental vasculature and fetal growth (Thomas et al., 2020). While GDM is typically diagnosed at 24-28 weeks, studying pregnancies affected by pregestational diabetes could provide insight into how early metabolic disturbances influence HBCs.

The placenta is a highly vascular organ and changes in placental vascular development in GDM placentae have been reported (Huynh et al., 2015). HBCs are anatomically positioned to influence villous angiogenesis, and their M2-like phenotype is compatible with pro-angiogenic and tissue remodelling roles. We observed strong positive correlations between HBC-enriched markers and the endothelial marker PECAM1/CD31 in both groups, consistent with earlier reports that HBCs can release angiogenic factors which assist endothelial network formation (Loegl et al., 2016). However, these relationships are correlative. Term placentae represent the end of gestation and do not permit inference regarding earlier developmental periods when angiogenic pathways are most active. Whilst one study in first trimester placentae, also reported a positive correlation between the number of vascular structures and HBCs (Seval et al., 2007), this correlation does not show causation, and further functional studies are needed to investigate this.

Macrophages are essential for preventing infection and HBCs have been shown to respond to inflammatory stimuli (Pantazi et al., 2022). If HBCs act in this manner, the observed reduction in HBC numbers in GDM placentae could potentially contribute to

an increased risk of fetal infection. Hyperglycaemia is known to impair innate immune responses outside pregnancy, by enhancing macrophage pro-inflammatory cytokine secretion and diminishing their phagocytic and pathogen-fighting abilities (Jafar et al., 2016). Notably, a reduction in HBC numbers is also observed in conditions like chorioamnionitis (Vinnars et al., 2010) and severe preeclampsia (Tang et al., 2013), which are associated with a higher risk of infection and neurodevelopmental *sequelae* in neonates (Beck et al., 2021; Rorman et al., 2020). Consistent with this notion, infants of GDM mothers are more likely to experience infectious morbidity (Zolotareva et al., 2022). Therefore, preserving both the quantity and anti-inflammatory properties of HBCs in GDM is likely vital for protecting the fetus and ensuring long-term offspring health. Although there has been some investigation into the role of HBCs in infection in normal pregnancies (Fakonti et al., 2022), studies specifically examining HBC responses to infection in GDM are lacking.

Despite these interesting findings, this study has some limitations. Because tissue was obtained from archived collections, the numbers of available samples, particularly for immunohistochemistry, remained modest. Moreover, glucose control data were not available, preventing assessment of the influence of glycaemic severity on HBCs. Finally, our work focused on HBC gene expression and abundance, rather than functional roles, and mechanistic implications cannot be inferred from these data. Functional studies across gestation are required to determine the biological significance of reduced HBC abundance.

In summary, our findings indicate that GDM is associated with reduced HBC abundance in terminal villi while preserving their M2-like phenotype. These alterations may contribute to the broader alterations in placental villous homeostasis observed in

GDM. Further mechanistic studies are needed to determine the developmental timing and functional impact of these changes.

**Acknowledgements**

GF is funded by a Leeds Doctoral Scholarship from University of Leeds. This work is supported by a Bioscientifica Trust Grant (GF) and grants from UK Research and Innovation (UKRI) and Medical Research Council (MR/R023166/1 and MR/Y003659/1). We thank the participants who donated their placentae, and staff in the delivery units that assisted with placentae collections. We gratefully acknowledge the Bio-imaging facility at University of Leeds, especially Dr Sally Boxall and Dr Ruth Hughes, for their support with slide scanner image acquisition.

**Data availability**

All data underlying the results are available as part of the article and no additional source data are required.

**References**

Alur, V., Raju, V., Vastrad, B., Tengli, A., Vastrad, C., Kottureshetti, S., 2021. Integrated bioinformatics analysis reveals novel key biomarkers and potential candidate small molecule drugs in gestational diabetes mellitus. Biosci Rep 41. https://doi.org/10.1042/BSR20210617

Bankhead, P., Loughrey, M.B., Fernández, J.A., Dombrowski, Y., McArt, D.G., Dunne, P.D., McQuaid, S., Gray, R.T., Murray, L.J., Coleman, H.G., James, J.A., Salto-Tellez, M., Hamilton, P.W., 2017. QuPath: Open source software for

digital pathology image analysis. Scientific Reports 2017 7:1 7, 1–7. https://doi.org/10.1038/s41598-017-17204-5

Beck, C., Gallagher, K., Taylor, L.A., Goldstein, J.A., Mithal, L.B., Gernand, A.D., 2021. Chorioamnionitis and Risk for Maternal and Neonatal Sepsis: A Systematic Review and Meta-analysis. Obstetrics and gynecology 137, 1007. https://doi.org/10.1097/AOG.0000000000004377

Bommarito, P.A., Cantonwine, D.E., Stevens, D.R., Welch, B.M., Davalos, A.D., Zhao, S., McElrath, T.F., Ferguson, K.K., 2023. Fetal growth trajectories of babies born large-for-gestational-age in the LIFECODES Fetal Growth Study. Am J Obstet Gynecol 228, 340.e1. https://doi.org/10.1016/J.AJOG.2022.10.006

Byford, A., Baird-Rayner, C., Forbes, K., 2021. Don’t sugar coat it: the effects of gestational diabetes on the placental vasculature. Biochem (Lond) 43, 34–39. https://doi.org/10.1042/BIO_2021_117

Byford, A.R., Fakonti, G., Shao, Z., Soni, S., Earle, S.L., Bajarwan, M., Morley, L.C., Holder, B., Scott, E.M., Forbes, K., 2025. Endothelial-to-mesenchymal transition in the fetoplacental macrovasculature and microvasculature in pregnancies complicated by gestational diabetes. J Physiol 1–21. https://doi.org/10.1113/JP287931

Chen, T., Liu, H.X., Yan, H.Y., Wu, D.M., Ping, J., 2016. Developmental origins of inflammatory and immune diseases. Mol Hum Reprod 22, 858. https://doi.org/10.1093/MOLEHR/GAW036

Clement, N.S., Abul, A., Farrelly, R., Murphy, H.R., Forbes, K., Simpson, N.A.B., Scott, E.M., 2024. Pregnancy outcomes in type 2 diabetes: a systematic review and meta-analysis. Am J Obstet Gynecol. https://doi.org/10.1016/J.AJOG.2024.11.026

Dairi, A.S., Himayda, A.S.A., Moulana, A.A.R., Bukhari, H.S.H., Hakeem, I.M., Elbarrany, W.G.E.A.E., 2020. The Effect of Gestational Diabetes Mellitus on the Chorionic Villi of Human Placenta Among Saudi Arabian Mothers: A Quantitative and Comparative Study. Cureus 12. https://doi.org/10.7759/CUREUS.11130

Depla, A.L., De Wit, L., Steenhuis, T.J., Slieker, M.G., Voormolen, D.N., Scheffer, P.G., De Heus, R., Van Rijn, B.B., Bekker, M.N., 2021. Effect of maternal diabetes on fetal heart function on echocardiography: systematic review and meta-analysis. Ultrasound Obstet Gynecol 57, 539–550. https://doi.org/10.1002/UOG.22163

Di Simone, N., Di Nicuolo, F., Marzioni, D., Castellucci, M., Sanguinetti, M., D'Lppolito, S., Caruso, A., 2008. Resistin modulates glucose uptake and glucose transporter-1 (GLUT-1) expression in trophoblast cells. J Cell Mol Med 13, 388. https://doi.org/10.1111/J.1582-4934.2008.00337.X

Di Simone, N., Di Nicuolo, F., Sanguinetti, M., Castellani, R., D'Asta, M., Caforio, L., Caruso, A., 2006. Resistin regulates human choriocarcinoma cell invasive behaviour and endothelial cell angiogenic processes. J Endocrinol 189, 691–699. https://doi.org/10.1677/JOE.1.06610

Erlich, A., Pearce, P., Mayo, R.P., Jensen, O.E., Chernyavsky, I.L., 2019. Physical and geometric determinants of transport in fetoplacental microvascular networks. Sci Adv 5. https://doi.org/10.1126/SCIADV.AAV6326/SUPPL_FILE/AAV6326_SM.PDF

Fakonti, G., Pantazi, P., Bokun, V., Holder, B., 2022. Placental Macrophage (Hofbauer Cell) Responses to Infection During Pregnancy: A Systematic Scoping Review. Front Immunol 12, 1–20. https://doi.org/10.3389/fimmu.2021.756035

Fetal Growth Calculator [WWW Document], n.d. URL https://srhr.org/fetalgrowthcalculator/#/ (accessed 9.17.24).

Hu, J., Ge, Z., Xu, Q., Shen, S., Wang, Y., Zhu, D., Bi, Y., 2020. Influence of fetal sex on perinatal outcomes in women with gestational diabetes mellitus. Diabetes Metab Res Rev 36, e3245. https://doi.org/10.1002/DMRR.3245

Huynh, J., Dawson, D., Roberts, D., Bentley-Lewis, R., 2015. A SYSTEMATIC REVIEW OF PLACENTAL PATHOLOGY IN MATERNAL DIABETES MELLITUS. Placenta 36, 101. https://doi.org/10.1016/J.PLACENTA.2014.11.021

Ingman, K., Cookson, V.J.K.W., Jones, C.J.P., Aplin, J.D., 2010. Characterisation of Hofbauer Cells in First and Second Trimester Placenta: Incidence, Phenotype, Survival in vitro and Motility. Placenta 31, 535–544. https://doi.org/10.1016/J.PLACENTA.2010.03.003

Jafar, N., Edriss, H., Nugent, K., 2016. The Effect of Short-Term Hyperglycemia on the Innate Immune System. Am J Med Sci 351, 201–211. https://doi.org/10.1016/J.AMJMS.2015.11.011

Kang, Y.E., Yi, H.S., Yeo, M.K., Kim, J.T., Park, D., Jung, Y., Kim, O.S., Lee, S.E., Kim, J.M., Joung, K.H., Lee, J.H., Ku, B.J., Lee, M., Kim, H.J., 2022. Increased Pro-Inflammatory T Cells, Senescent T Cells, and Immune-Check Point Molecules in the Placentas of Patients With Gestational Diabetes Mellitus. J Korean Med Sci 37. https://doi.org/10.3346/JKMS.2022.37.E338

Kerby, A., Shingleton, D., Batra, G., Sharps, M.C., Baker, B.C., Heazell, A.E.P., 2021. Placental morphology and cellular characteristics in stillbirths in women with diabetes and unexplained stillbirths. Arch Pathol Lab Med 145, 82–89. https://doi.org/10.5858/arpa.2019-0524-OA

Kim, S.Y., Romero, R., Tarca, A.L., Bhatti, G., Kim, C.J., Lee, J., Elsey, A., Than, N.G., Chaiworapongsa, T., Hassan, S.S., Kang, G.H., Kim, J.S., 2012. Methylome of Fetal and Maternal Monocytes and Macrophages at the Feto-Maternal Interface. Am J Reprod Immunol 68, 8. https://doi.org/10.1111/J.1600-0897.2012.01108.X

Kiserud, T., Benachi, A., Hecher, K., Perez, R.G., Carvalho, J., Piaggio, G., Platt, L.D., 2018. The World Health Organization fetal growth charts: concept, findings, interpretation, and application. Am J Obstet Gynecol 218, S619–S629. https://doi.org/10.1016/J.AJOG.2017.12.010

Koru-Sengul, T., Santander, A.M., Miao, F., Sanchez, L.G., Jorda, M., Glück, S., Ince, T.A., Nadji, M., Chen, Z., Penichet, M.L., Cleary, M.P., Torroella-Kouri, M., 2016. Breast cancers from black women exhibit higher numbers of immunosuppressive macrophages with proliferative activity and of crown-like structures associated with lower survival compared to non-black Latinas and Caucasians. Breast Cancer Res Treat 158, 113. https://doi.org/10.1007/S10549-016-3847-3

Lacagnina, S., 2019. The Developmental Origins of Health and Disease (DOHaD). Am J Lifestyle Med 14, 47. https://doi.org/10.1177/1559827619879694

Law, G.R., Ellison, G.T.H., Secher, A.L., Damm, P., Mathiesen, E.R., Temple, R., Murphy, H.R., Scott, E.M., 2015. Analysis of Continuous Glucose Monitoring in Pregnant Women With Diabetes: Distinct Temporal Patterns of Glucose Associated With Large-for-Gestational-Age Infants. Diabetes Care 38, 1319–1325. https://doi.org/10.2337/DC15-0070

463 Leach, L., Taylor, A., Sciota, F., 2009. Vascular dysfunction in the diabetic
464 placenta: Causes and consequences. J Anat 215, 69–76.
465 https://doi.org/10.1111/j.1469-7580.2009.01098.x
466 Li, S., Zhu, Y., Yeung, E., Chavarro, J.E., Yuan, C., Field, A.E., Missmer, S.A.,
467 Mills, J.L., Hu, F.B., Zhang, C., 2017. Offspring risk of obesity in childhood,
468 adolescence and adulthood in relation to gestational diabetes mellitus: a sex-
469 specific association. Int J Epidemiol 46, 1533–1541.
470 https://doi.org/10.1093/IJE/DYX151
471 Loegl, J., Hiden, U., Nussbaumer, E., Schliefsteiner, C., Cvitic, S., Lang, I.,
472 Wadsack, C., Huppertz, B., Desoye, G., 2016. Hofbauer cells of M2a, M2b and
473 M2c polarization may regulate feto-placental angiogenesis. Reproduction 152,
474 447–455. https://doi.org/10.1530/REP-16-0159
475 Lu, S., Wang, J., Kakongoma, N., Hua, W., Xu, J., Wang, Y., He, S., Gu, H., Shi,
476 J., Hu, W., 2022. DNA methylation and expression profiles of placenta and
477 umbilical cord blood reveal the characteristics of gestational diabetes mellitus
478 patients and offspring. Clin Epigenetics 14, 1–16.
479 https://doi.org/10.1186/S13148-022-01289-5/FIGURES/4
480 Mahadevan, A., Tipler, A., Jones, H., 2023. Shared developmental pathways of
481 the placenta and fetal heart. Placenta 141, 35–42.
482 https://doi.org/10.1016/J.PLACENTA.2022.12.006
483 Mallardo, M., Ferraro, S., Daniele, A., Nigro, E., 2021. GDM-complicated
484 pregnancies: focus on adipokines. Mol Biol Rep 48, 8171–8180.
485 https://doi.org/10.1007/S11033-021-06785-0
486 Mrizak, I., Grissa, O., Henault, B., Fekih, M., Bouslema, A., Boumaiza, I.,
487 Zaouali, M., Tabka, Z., Khan, N.A., 2014. Placental infiltration of inflammatory

markers in gestational diabetic women. Gen Physiol Biophys 33, 169–176. https://doi.org/10.4149/GPB_2013075

Murray, S.R., Reynolds, R.M., 2020. Short- and long-term outcomes of gestational diabetes and its treatment on fetal development. Prenat Diagn 40, 1085–1091. https://doi.org/10.1002/PD.5768

Nandy, D., Janardhanan, R., Mukhopadhyay, D., Basu, A., 2011. Effect of Hyperglycemia on Human Monocyte Activation. J Investig Med 59, 661. https://doi.org/10.231/JIM.0B013E31820EE432

Nielsen, G.L., Dethlefsen, C., Lundbye-Christensen, S., Pedersen, J.F., Mølsted-Pedersen, L., Gillman, M.W., 2012. Adiposity in 277 young adult male offspring of women with diabetes compared with controls: A Danish population-based cohort study. Acta Obstet Gynecol Scand 91, 838. https://doi.org/10.1111/J.1600-0412.2012.01413.X

Owen, M.D., Kennedy, M.G., Quilang, R.C., Scott, E.M., Forbes, K., 2024. The role of microRNAs in pregnancies complicated by maternal diabetes. Clin Sci 138, 1179–1207. https://doi.org/10.1042/CS20230681

Pantazi, P., Kaforou, M., Tang, Z., Abrahams, V.M., McArdle, A., Guller, S., Holder, B., 2022. Placental macrophage responses to viral and bacterial ligands and the influence of fetal sex. iScience 25, 105653. https://doi.org/10.1016/J.ISCI.2022.105653

Radaelli, T., Varastehpour, A., Catalano, P., Hauguel-De Mouzon, S., 2003. Gestational diabetes induces placental genes for chronic stress and inflammatory pathways. Diabetes 52, 2951–2958. https://doi.org/10.2337/DIABETES.52.12.2951

512 Retnakaran, R., Shah, B.R., 2015. Fetal Sex and the Natural History of Maternal
513 Risk of Diabetes During and After Pregnancy. J Clin Endocrinol Metab 100,
514 2574–2580. https://doi.org/10.1210/JC.2015-1763
515 Reyes, L., Golos, T.G., 2018. Hofbauer Cells: Their Role in Healthy and
516 Complicated Pregnancy. Front Immunol 9, 2628.
517 https://doi.org/10.3389/fimmu.2018.02628
518 Rorman, E., Freud, A., Wainstock, T., Sheiner, E., 2020. Maternal preeclampsia
519 and long-term infectious morbidity in the offspring – A population based cohort
520 analysis. Pregnancy Hypertens 21, 30–34.
521 https://doi.org/10.1016/J.PREGHY.2020.04.010
522 Schliefsteiner, C., Peinhaupt, M., Kopp, S., Lögl, J., Lang-Olip, I., Hiden, U.,
523 Heinemann, A., Desoye, G., Wadsack, C., 2017. Human Placental Hofbauer
524 Cells Maintain an Anti-inflammatory M2 Phenotype despite the Presence of
525 Gestational Diabetes Mellitus. Front Immunol 8.
526 https://doi.org/10.3389/FIMMU.2017.00888
527 Scott, E.M., Murphy, H.R., Kristensen, K.H., Feig, D.S., Kjolhede, K., Englund-
528 Ogge, L., Berntorp, K.E., Law, G.R., 2022. Continuous Glucose Monitoring
529 Metrics and Birth Weight: Informing Management of Type 1 Diabetes
530 Throughout Pregnancy. Diabetes Care 45, 1724–1734.
531 https://doi.org/10.2337/DC22-0078
532 Seval, Y., Korgun, E.T., Demir, R., 2007. Hofbauer Cells in Early Human
533 Placenta: Possible Implications in Vasculogenesis and Angiogenesis. Placenta
534 28, 841–845. https://doi.org/10.1016/j.placenta.2007.01.010
535 Tang, Z., Buhimschi, I.A., Buhimschi, C.S., Tadesse, S., Norwitz, E., Niven-
536 Fairchild, T., Huang, S.T.J., Guller, S., 2013. Decreased Levels of Folate

Receptor-β and Reduced Numbers of Fetal Macrophages (Hofbauer Cells) in Placentas from Pregnancies with Severe Pre-Eclampsia. American Journal of Reproductive Immunology 70, 104–115. https://doi.org/10.1111/AJI.12112

Thomas, J., Appios, A., Zhao, X., Dutkiewicz, R., Donde, M., Lee, Colin, Naidu, P., Lee, Christopher, Cerveira, J., Liu, B., Ginhoux, F., Burton, G., Hamilton, R.S., Moffett, A., Sharkey, A., McGovern, N., 2020. Phenotypic and functional characterisation of first trimester human placental macrophages, Hofbauer cells. Journal of Experimental Medicine 218, 1–17. https://doi.org/10.1101/2020.09.03.279919

Vinnars, M.T.N., Rindsjö, E., Ghazi, S., Sundberg, A., Papadogiannakis, N., 2010. The number of CD68(+) (Hofbauer) cells is decreased in placentas with chorioamnionitis and with advancing gestational age. Pediatr Dev Pathol 13, 300–304. https://doi.org/10.2350/09-03-0632-OA.1

Ye, W., Luo, C., Huang, J., Li, C., Liu, Z., Liu, F., 2022. Gestational diabetes mellitus and adverse pregnancy outcomes: systematic review and meta-analysis. BMJ 377. https://doi.org/10.1136/BMJ-2021-067946

Yoshida, N., Appios, A., Li, Q., Hutton, J.P., Wood, G., Potts, M., Aleksandrowicz, J., Barrozo, E.R., Dover, F., Anderson, H., Stephens, K., Aye, I.L.M.H., Thomas, J.R., Schenk, H.C.M., Bourke, A.M., Aiken, C.E., Moffett, A., Sharkey, A., Protasio, A. V., Aagaard, K.M., Edgar, J.R., Chung, B.Y.W., McGovern, N., 2025. Interactions between placental Hofbauer cells and L. monocytogenes change throughout gestation. Sci Immunol 10, 3066. https://doi.org/10.1126/SCIIMMUNOL.ADQ3066

Yu, J., Zhou, Y., Gui, J., Li, A.Z., Su, X.L., Feng, L., 2013. Assessment of the number and function of macrophages in the placenta of gestational diabetes

562 mellitus patients. J Huazhong Univ Sci Technolog Med Sci 33, 725–729.
563 https://doi.org/10.1007/S11596-013-1187-7
564 Zhang, M., Cui, D., Yang, H., 2022. The Distributional Characteristics of M2
565 Macrophages in the Placental Chorionic Villi are Altered Among the Term
566 Pregnant Women With Uncontrolled Type 2 Diabetes Mellitus. Front Immunol
567 13, 1005. https://doi.org/10.3389/FIMMU.2022.837391/BIBTEX
568 Zolotareva, V., Sheiner, E., Sergienko, R., Wainstock, T., 2022. Gestational
569 Diabetes Mellitus and Offspring Infectious Morbidities- A Sibling Analysis. Am J
570 Obstet Gynecol 226, S588–S589. https://doi.org/10.1016/j.ajog.2021.11.972
571
572

573 **Tables**

574 **Table 1: Antibodies used in immunohistochemistry experiments.**
575

| **Primary antibodies** | | | |
|---|---|---|---|
| **Target** | **Host species** | **Final concentration** | **Manufacturer (catalogue number) (*clone number)* (*RRID number)*** |
| CD163 | Rabbit | 0.96 µg/ml | Abcam (ab182422) *(EPR19518)* *(RRID: AB_2753196)* |
| CD68 | Rabbit | 0.79 µg/ml | Abcam (ab213363) *(EPR20545)* *(RRID:AB_2801637)* |
| CD86 | Mouse | 2 µg/ml | Abcam (ab220188) *(C86/1146)* *(-)* |
| MRC1 | Mouse | 0.2 µg/ml | Proteintech (60143-1-Ig) *(2A6A10)* *(RRID:AB_2144924)* |
| **Secondary antibodies and IgG control** | | | |
| **Antibody** | **Host species** | **Dilution** | **Manufacturer (catalogue number) (*clone number)* (*RRID number*** |
| Biotinylated anti mouse IgG | Goat | 5 µg/ml | AAT Bioquest (16729) *(-)* *(-)* |
| Biotinylated anti rabbit IgG | Swine | 2.55 µg/ml | Dako (E0353) *(-)* *(RRID:AB_2737292)* |
| Rabbit IgG control | Rabbit | Relative to primary antibody | Vector Laboratories (I-1000) *(-)* *(RRID:AB_2336355)* |

576
577

578
579 **Table 2: List of primers for target and housekeeping genes.**
580

| Target gene | Direction | Sequence (5'->3') | Annealing temperature (°C) |
|---|---|---|---|
| CD68 | Forward | CGAGCATCATTCTTTCACCAGCT | 60 |
| | Reverse | ATGAGAGGCAGCAAGATGGACC | |
| CD14 | Forward | CTGGAACAGGTGCCTAAAGGAC | 60 |
| | Reverse | GTCCAGTGTCAGGTTATCCACC | |
| CD163 | Forward | CGGTCTCTGTGATTTGTAACCAG | 55 |
| | Reverse | TACTATGCTTTCCCCATCCATC | |
| MRC1 | Forward | GACGTGGCTGTGGATAAATAAC | 55 |
| | Reverse | CAGAAGACGCATGTAAAGCTAC | |
| FOLR2 | Forward | CCTGTACCGAAGACAGAGGC | 60 |
| | Reverse | GAGCTGAACCTCCGTTGCT | |
| VSIG4 | Forward | AGAGAGTGTAACAGGACCTT | 55 |
| | Reverse | GTCACGTAGAAAGATGGTGA | |
| PECAM1 (CD31) | Forward | GCTGAGTCTCACAAAGATCTAGGA | 57 |
| | Reverse | ATCTGCTTTCCACGGCATCA | |
| **Housekeeping gene** | **Direction** | **Sequence (5'->3')** | **Annealing temperature (°C)** |
| YWHAZ | Forward | ACTTTTGGTACATTGTGGCTTCAA | 55 |
| | Reverse | CCGCCAGGACAAACCAGTAT | |
| GUSB | Forward | GTCTGCGGCATTTTGTCGG | 55 |
| | Reverse | CACACGATGGCATAGGAATGG | |
| RPLP0 | Forward | AGCCCAGAACACTGGTCTC | 55 |
| | Reverse | ACTCAGGATTTCAATGGTGCC | |

**Table 3: Demographics of placental samples with/without GDM included in the RT-qPCR and immunohistochemistry experiments.**

| RT-qPCR | | | | Immunohistochemistry | | | |
|---|---|---|---|---|---|---|---|
| | **Non-GDM (n=18)** | **GDM (n=19)** | **p-value** | | **Non-GDM (n=13)** | **GDM (n=12)** | **p-value** |
| **Maternal age (years)[1]** | 29.8 ± 5.26 | 32.5 ± 4.05 | 0.09 | **Maternal age (years)[1]** | 31.3 ± 5.59 | 29.8 ± 6.81 | 0.56 |
| **Booking BMI (kg/m$^2$)[1]** | 29.1 ± 8.66 | 30.4 ± 5.86 [a] | 0.61 | **Booking BMI (kg/m$^2$)[3]** | 28.2 (27.3 30.2) | 33.8 (29.4, 35.5)[c] | 0.06 |
| **Ethnicity[2]** | | | 0.12 | **Ethnicity[2]** | | | 0.32 |
| White | 13 (72.2) | 9 (47.4) | | White | 11 (84.6) | 6 (50.0) | |
| Black | 1 (5.6) | 0 (0.0) | | Black | 0 (0.0) | 1 (8.3) | |
| Asian | 4 (22.2) | 7 (36.8) | | Asian | 1 (7.7) | 3 (25.0) | |
| Other | 0 (0.0) | 3 (15.8) | | Other | 1 (7.7) | 2 (16.7) | |
| **Smoking status[2]** | | | 0.23 | **Smoking status[2]** | | | 0.21 |
| QDP | 1 (5.6) | 0 (0.0) | | | 4 (30.8) | 0 (0.0) | |
| Non-smoker | 16 (88.9) | 19 (100.0) | | Ex-smoker | 7 (53.8) | 9 (75.0) | |
| Smoker | 1 (5.6) | 0 (0.0) | | Non-smoker | 1 (7.7) | 1 (8.3) | |
| | | | | Smoker | 1 (7.7) | 2 (16.7) | |
| | | | | Unknown | | | |
| **Gestational age (days)[1]** | 274.2 ± 6.93 | 270.9 ± 6.32 [b] | 0.15 | **Gestational age (days)[3]** | 275 (273, 277) | 274 (272, 277) | 0.51 |
| **Parity[2]** | | | 0.55 | **Parity[2]** | | | 0.25 |
| 0 | 5 (27.8) | 4 (21.1) | | 0 | 2 (15.4) | 5 (41.7) | |
| 1 | 6 (33.3) | 7 (36.8) | | 1 | 5 (38.4) | 6 (50.0) | |
| 2 | 5 (27.8) | 3 (15.8) | | 2 | 4 (30.8) | 1 (8.3) | |
| 3 | 2 (11.1) | 2 (10.5) | | 3 | 1 (7.7) | 0 (0.0) | |
| ≥4 | 0 (0.0) | 3 (15.8) | | ≥4 | 1 (7.7) | 0 (0.0) | |
| **Mode of delivery[2]** | | | 0.12 | **Mode of delivery[2]** | | | 0.122 |
| SVD | 6 (33.3) | 4 (21.1) | | SVD | 0 (0.0) | 2 (16.7) | |
| VD-ind | 0 (0.0) | 2 (10.5) | | CS-el | 13 (100.0) | 10 (83.3) | |
| CS-el | 11 (61.1) | 8 (42.1) | | | | | |
| CS-em | 0 (0.0) | 4 (21.2) | | | | | |
| Unknown | 1 (5.6) | 1 (5.2) | | | | | |
| **Placental weight (g)[1]** | 622.2 ± 140.5 [b] | 664.6 ± 250 | 0.54 | **Placental weight (g)[1]** | 562 ± 131[d] | 758 ± 239 | **0.02** |
| **Birthweight (g)[1]** | 3816 ± 479.8 | 3725 ± 612.6 | 0.62 | **Birthweight (g)[1]** | 3715 ± 566 | 3840 ± 409 | 0.53 |
| **Fetal: placental weight ratio[3]** | 6.1 (4.7, 6.9)[b] | 5.6 (4.9, 6.8) | 0.16 | **Fetal: placental weight ratio[3]** | 6.9 (6.0, 7.5)[d] | 4.6 (4.3, 6.5) | **0.01** |
| **Fetal sex[2]** | | | >0.99 | **Fetal sex[2]** | | | 0.43 |
| Male | 10 (55.6) | 9 (47.4) | | Male | 9 (69.2) | 6 (50.0) | |
| Female | 8 (44.4) | 9 (47.4) | | Female | 4 (30.8) | 6 (50.0) | |
| Unknown | 0 (0.0) | 1 (5.2) | | | | | |

[1]mean ± standard deviation, [2]frequency (%), [3]median (q1, q2), [a]n=18, [b]n=17, [c]n=10, [d]n=15, QDP; quit during pregnancy, SVD; spontaneous vaginal delivery, VD-ind; induced vaginal delivery, CS-el; elective caesarean section, CS-em; emergency caesarean section. Statistical significance at the 0.05 level.

590 **Figure legends**

591

592 **Figure 1: Gene expression of HBC- and macrophage- enriched markers in non-**
593 **GDM and GDM human placental tissue.**

594 *Gene expression of the (**A**) pan-macrophage- (CD14 and CD68), (**B**) M2- (CD163 and*
595 *MRC1), and (**C**) HBC-enriched (FOLR2 and VSIG4) markers. Data presented as*
596 *median with interquartile range and analysed by Mann-Whitney test (two-tailed)*
597 *(CD14; p-value=0.77, CD163; p-value=0.01, MRC1; p-value=0.12, FOLR2; p-*
598 *value=0.03) or mean with SD and analysed by unpaired t-test (two-tailed) (CD68; p-*
599 *value=0.10, VSIG4; p-value=0.03). Non-GDM (n=18) and GDM (n=19). p-value*
600 *<0.05*, ≤0.01**. Expression was normalised to the average of YWHAZ, RPLP0, and*
601 *GUSB.*

602 ***Figure 2: Immunohistochemistry analysis of placental tissue from non-GDM***
603 ***and GDM pregnancies.***

604 *HBCs positive for (A) the pan-macrophage (CD68), (B-C) M2 (CD163, MRC1), and*
605 *(**D**) HBC-enriched (FOLR2) markers were identified in different locations within the*
606 *chorionic villi of the placenta in both non-GDM and GDM pregnancies. Negative*
607 *controls (secondary antibody only or IgG controls were used). (**E**) HBCs were*
608 *negative for the M1 marker CD86. (**F**) Human uterine samples were used as a*
609 *positive control (CD86 staining on the left and negative control on the right). Scale*
610 *bar: 50μm. Non-GDM (n=13) and GDM (n=12). Bold indicates statistical significance*
611 *at the 0.05 level, p-value <0.05*, p-value ≤0.01**, p-value ≤0.001***.*

**Figure 3: mRNA expression of HBC- and macrophage- enriched markers and immunohistochemistry analysis of placental tissue classified by pathological fetal growth or sex and diabetes status.**

*(**A**) Data presented as mean with SD and analysed by two-way ANOVA, with results displayed in tables. Expression is normalised to YWHAZ, GUSB, and RPLP0 expression. Non-GDM/AGA (n=8), non-GDM/LGA (n=8), GDM/AGA (n=11), and GDM/LGA (n=8), non-GDM/Female (n=6), non-GDM/male (n=6), GDM/female (n=6), and GDM/male (n=6). (**B**) Analysis of positive cells per surface area between non-GDM and GDM samples classified by fetal growth and by fetal sex. Data presented as mean with SD and analysed using two-way ANOVA. Non-GDM/AGA (n=9), non-GDM/LGA (n=8), GDM/AGA (n=6), and GDM/LGA (n=6), non-GDM/female (n=4), non-GDM/male (n=4), GDM/female (n=4), and GDM/male (n=4). AGA: appropriate for gestational age, LGA: large for gestational age. Bold indicates statistical significance at the 0.05 level, p-value <0.05*, p-value ≤0.01**, p-value ≤0.001***.*

**Figure 4: HBCs in placental vascular development.**

***(A)*** *HBCs are found in different locations within the chorionic villi of the placenta in both normal and GDM placentae. Representative image from GDM placenta using the pan-macrophage marker CD68 (same observations were also made in non-GDM placentae and with staining for FOLR2, MRC1, and CD163). Red arrows indicate areas presented in detail (right) Scale bar: 100μm and details scale bar: 10μm. BV: blood vessel. (**B-C**) Correlation matrix of the gene expression of pan-macrophage (CD14, CD68), M2 (CD163, MRC1), HBC-enriched markers with the expression of vascular marker, CD31 (also known as PECAM1). Numeric value in each square represents the Pearson's*

*correlation coefficient (colour and numeric value between -1; orange to 1; blue) for (**B**) non-GDM samples (n=17) and (**C**) GDM samples (n=18). Significant correlation is represented with red asterisks within each square p-value <0.05*, ≤0.01**, ≤0.001***.*

**Figure 1**

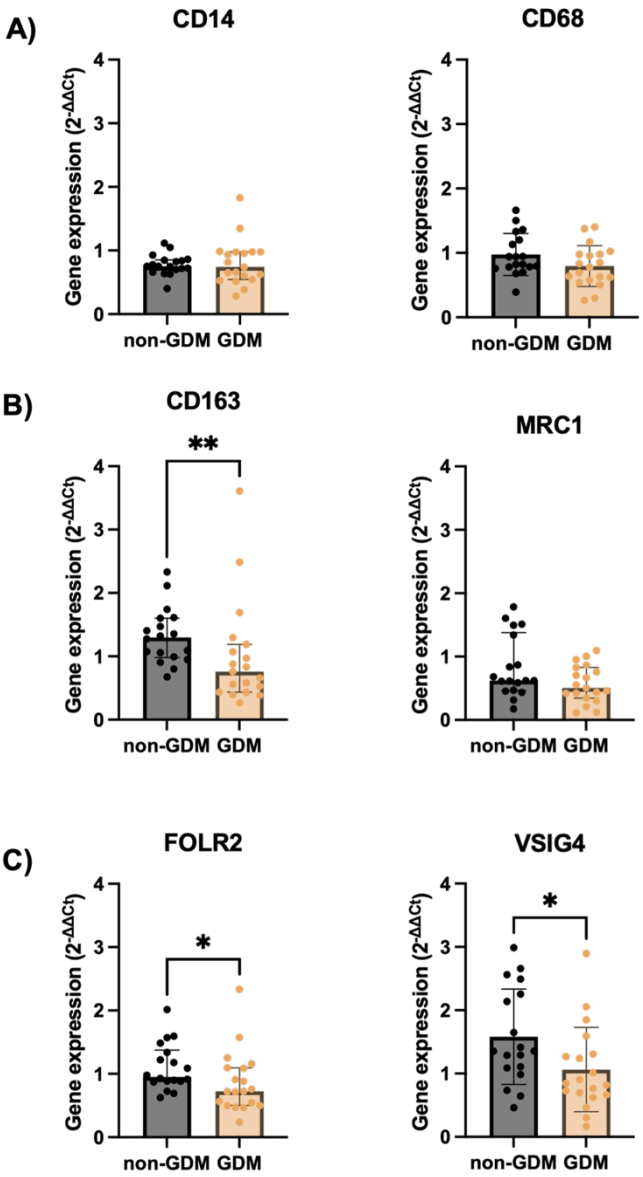

663 **Figure 2**

664

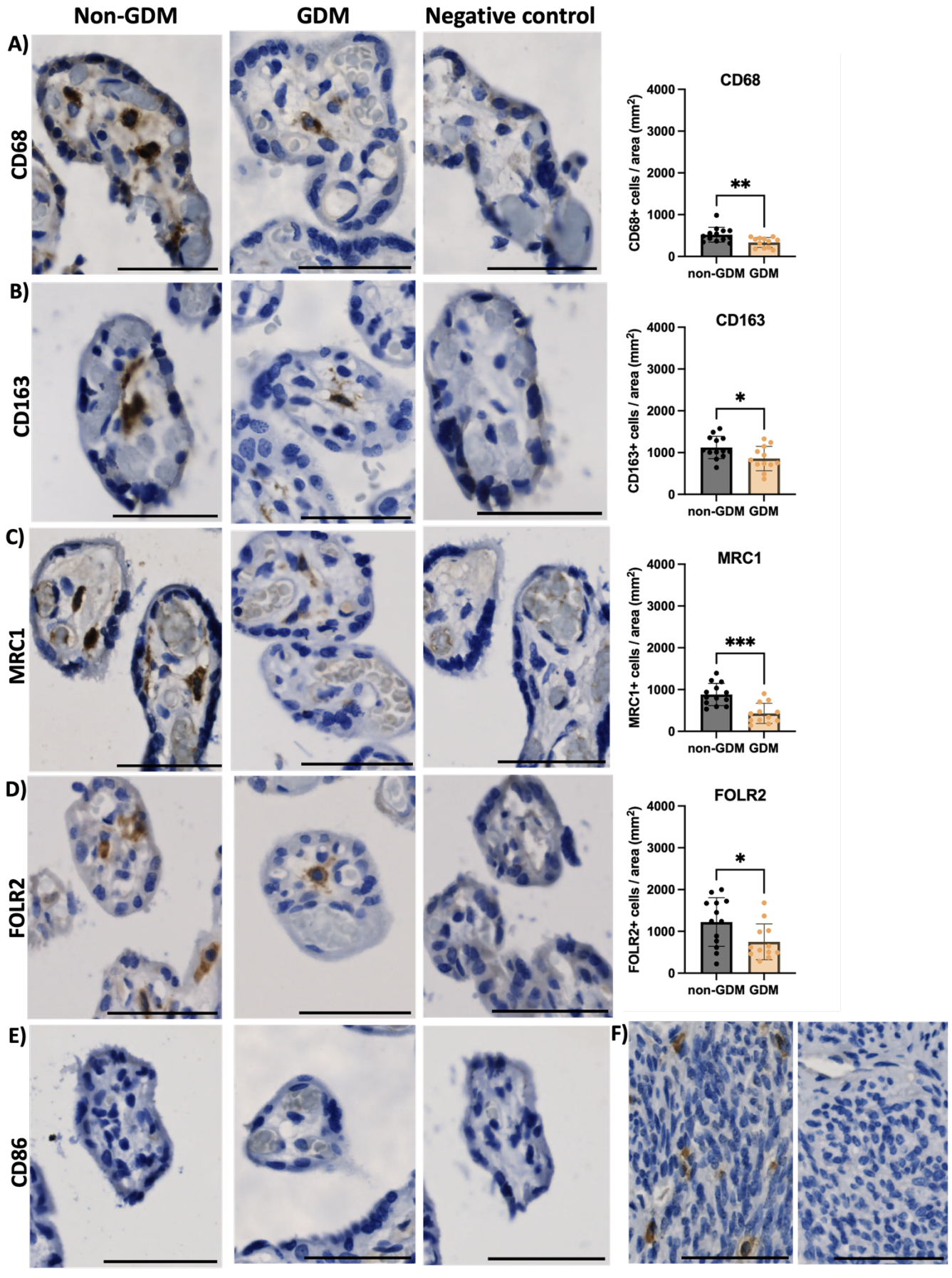
Non-GDM
GDM
Negative control
A)
CD68
CD68
CD68+ cells / area (mm²)
4000
3000
2000
1000
0
**
non-GDM GDM
B)
CD163
CD163
CD163+ cells / area (mm²)
*
C)
MRC1
MRC1
MRC1+ cells / area (mm²)
***
D)
FOLR2
FOLR2
FOLR2+ cells / area (mm²)
*
E)
CD86
F)

665
666

## Figure 3

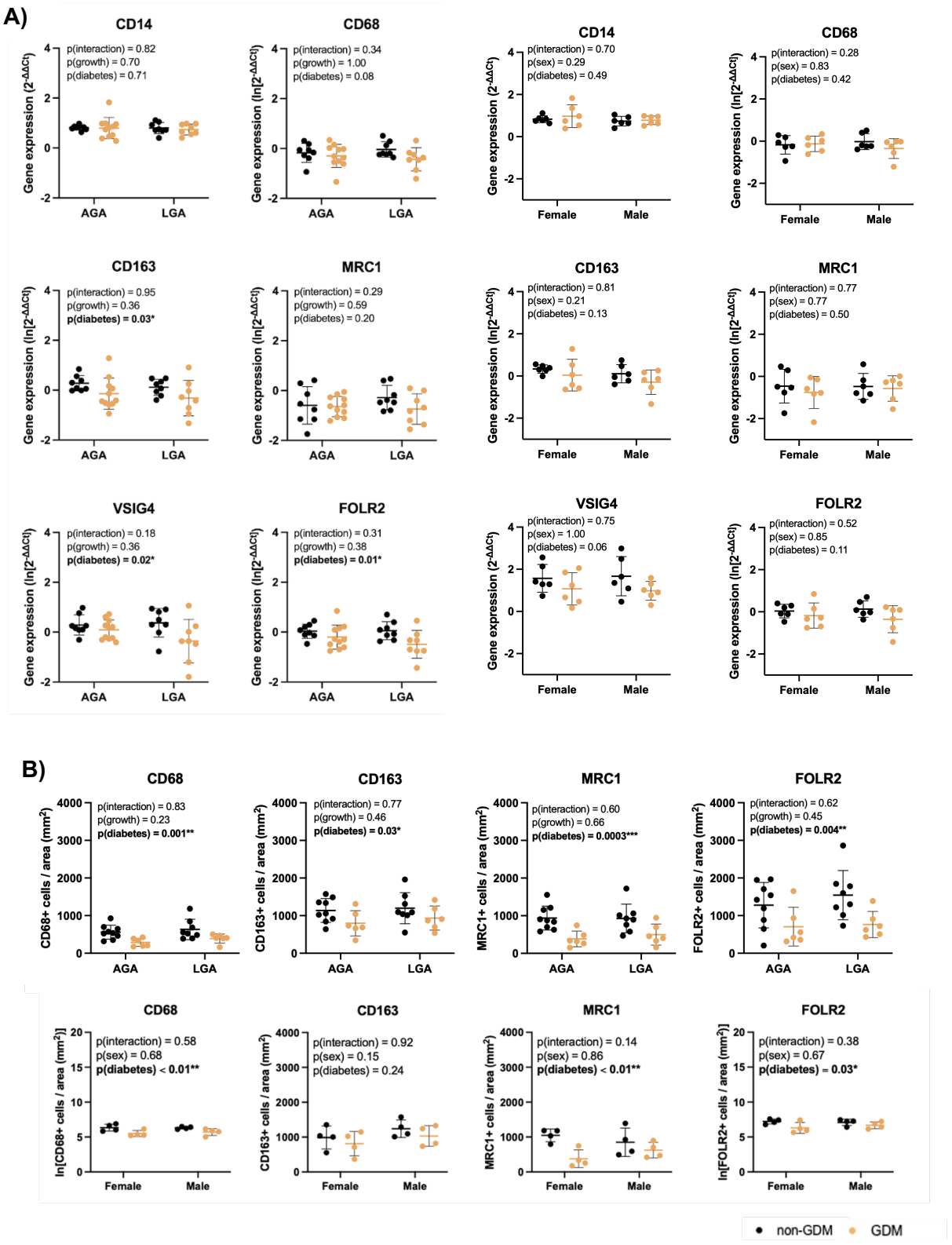
A)
CD14
p(interaction) = 0.82
p(growth) = 0.70
p(diabetes) = 0.71
CD68
p(interaction) = 0.34
p(growth) = 1.00
p(diabetes) = 0.08
CD14
p(interaction) = 0.70
p(sex) = 0.29
p(diabetes) = 0.49
CD68
p(interaction) = 0.28
p(sex) = 0.83
p(diabetes) = 0.42
CD163
p(interaction) = 0.95
p(growth) = 0.36
p(diabetes) = 0.03*
MRC1
p(interaction) = 0.29
p(growth) = 0.59
p(diabetes) = 0.20
CD163
p(interaction) = 0.81
p(sex) = 0.21
p(diabetes) = 0.13
MRC1
p(interaction) = 0.77
p(sex) = 0.77
p(diabetes) = 0.50
VSIG4
p(interaction) = 0.18
p(growth) = 0.36
p(diabetes) = 0.02*
FOLR2
p(interaction) = 0.31
p(growth) = 0.38
p(diabetes) = 0.01*
VSIG4
p(interaction) = 0.75
p(sex) = 1.00
p(diabetes) = 0.06
FOLR2
p(interaction) = 0.52
p(sex) = 0.85
p(diabetes) = 0.11
Gene expression (2-ΔΔCt)
Gene expression (ln[2-ΔΔCt])
AGA
LGA
Female
Male
B)
CD68
p(interaction) = 0.83
p(growth) = 0.23
p(diabetes) = 0.001**
CD163
p(interaction) = 0.77
p(growth) = 0.46
p(diabetes) = 0.03*
MRC1
p(interaction) = 0.60
p(growth) = 0.66
p(diabetes) = 0.0003***
FOLR2
p(interaction) = 0.62
p(growth) = 0.45
p(diabetes) = 0.004**
CD68+ cells / area (mm2)
CD163+ cells / area (mm2)
MRC1+ cells / area (mm2)
FOLR2+ cells / area (mm2)
CD68
p(interaction) = 0.58
p(sex) = 0.68
p(diabetes) < 0.01**
CD163
p(interaction) = 0.92
p(sex) = 0.15
p(diabetes) = 0.24
MRC1
p(interaction) = 0.14
p(sex) = 0.86
p(diabetes) < 0.01**
FOLR2
p(interaction) = 0.38
p(sex) = 0.67
p(diabetes) = 0.03*
ln[CD68+ cells / area (mm2)]
ln[FOLR2+ cells / area (mm2)]
non-GDM
GDM

**Figure 4**

A)

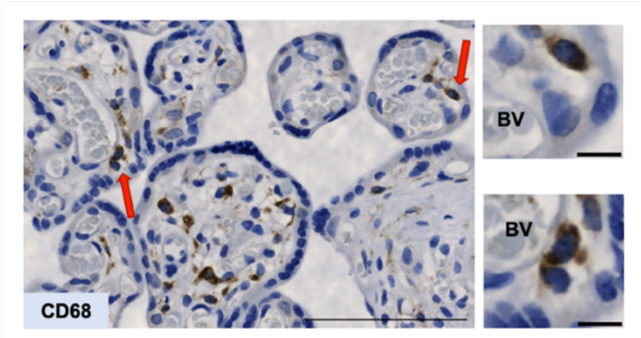
CD68
BV
BV

B)

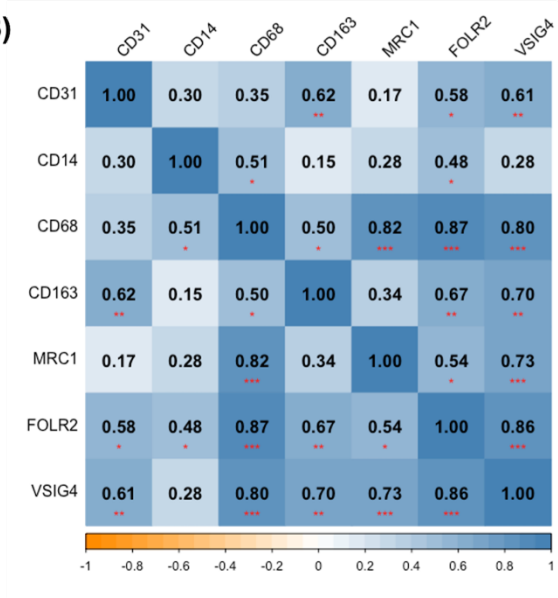
CD31 CD14 CD68 CD163 MRC1 FOLR2 VSIG4
CD31 1.00 0.30 0.35 0.62 0.17 0.58 0.61
CD14 0.30 1.00 0.51 0.15 0.28 0.48 0.28
CD68 0.35 0.51 1.00 0.50 0.82 0.87 0.80
CD163 0.62 0.15 0.50 1.00 0.34 0.67 0.70
MRC1 0.17 0.28 0.82 0.34 1.00 0.54 0.73
FOLR2 0.58 0.48 0.87 0.67 0.54 1.00 0.86
VSIG4 0.61 0.28 0.80 0.70 0.73 0.86 1.00
-1 -0.8 -0.6 -0.4 -0.2 0 0.2 0.4 0.6 0.8 1

C)

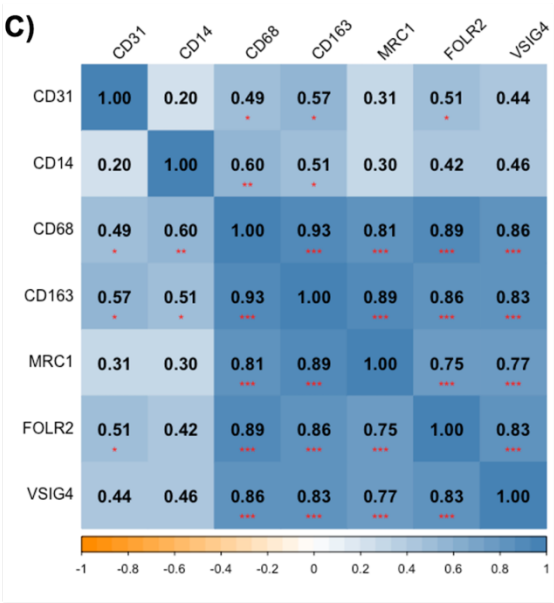
CD31 CD14 CD68 CD163 MRC1 FOLR2 VSIG4
CD31 1.00 0.20 0.49 0.57 0.31 0.51 0.44
CD14 0.20 1.00 0.60 0.51 0.30 0.42 0.46
CD68 0.49 0.60 1.00 0.93 0.81 0.89 0.86
CD163 0.57 0.51 0.93 1.00 0.89 0.86 0.83
MRC1 0.31 0.30 0.81 0.89 1.00 0.75 0.77
FOLR2 0.51 0.42 0.89 0.86 0.75 1.00 0.83
VSIG4 0.44 0.46 0.86 0.83 0.77 0.83 1.00
-1 -0.8 -0.6 -0.4 -0.2 0 0.2 0.4 0.6 0.8 1

## Supplementary materials

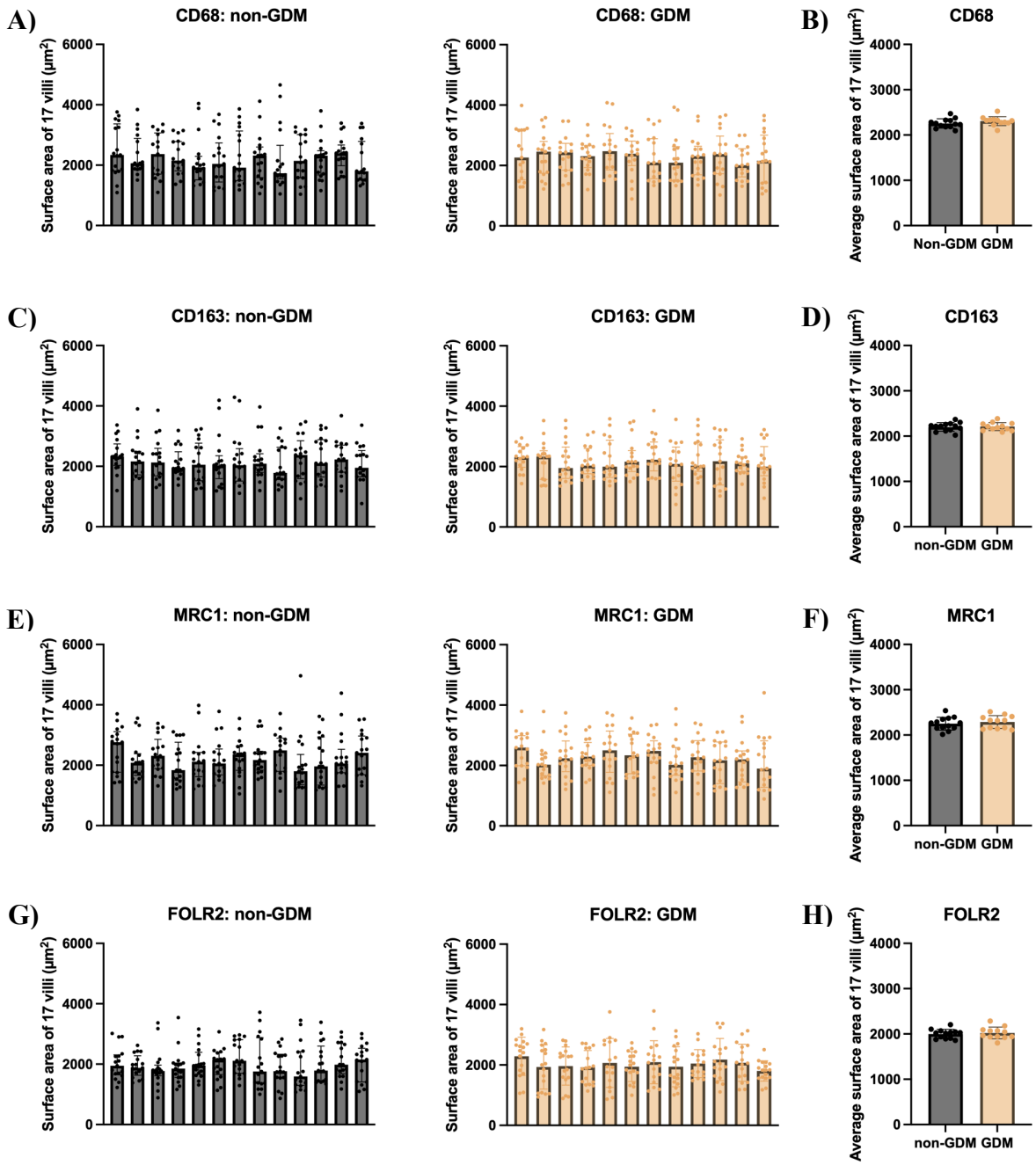


**Supplementary Figure 1: Comparable villous surface areas between participants in the non-GDM and GDM groups.**

*(**A-H**) The selected surface area of 17 villi per sample was comparable across samples within the non-GDM and GDM group and average area for each participant was comparable across the two groups. (**A**) For CD68 analysis, data are presented as median with interquartile range and analysed by Kruskal-Wallis with Dunn's post hoc test (non-GDM; p=0.85, GDM; 0.98) and (**B**) for average area comparison, data presented as mean with SD and analysed by unpaired t-test (two-tailed) (CD68; p=0.21). (**C**) For CD163 analysis, data are presented as median with interquartile range and analysed by Kruskal-Wallis with Dunn's post hoc test (non-GDM; p=0.97, GDM; p=0.98) and (**D**) for average area comparison, data are presented as mean with SD and analysed by unpaired t-test (two-tailed) (CD163; p=0.85). (**E**) For MRC1 analysis, data are presented as median with interquartile range and analysed by Kruskal-Wallis with Dunn's post hoc test (non-GDM; p=0.50, GDM; p=0.59) and (**F**) for average area comparison, data are presented as mean with SD and analysed by unpaired t-test (two-tailed) (MRC1; p=0.52). (**G**) For FOLR2 analysis of non-GDM samples, data are presented as median with interquartile range and analysed by Kruskal-Wallis with Dunn's post hoc test (p=0.79) and for GDM samples as mean with SD*

*and analysed by one-way ANOVA with Tukey post hoc test (p=0.74) and (**H**) for average area comparison, data are presented as mean with SD and analysed by unpaired t-test (two-tailed) (p=0.66). (**A**,**C**,**E**,**G**) Each bar represents a different sample and dots represent surface area of villi (μm$^2$). Non-GDM (n=13) and GDM (n=12).*

**Supplementary Table 1: Demographics of placental samples with/without GDM and pathological fetal growth used for the RT-qPCR experiments.**

| | Non-GDM AGA (n=8) | Non-GDM LGA (n=8) | GDM AGA (n=11) | GDM LGA (n=8) | p-value |
|---|---|---|---|---|---|
| **Maternal age (years)**[1] | 28.4± 6.97 | 31.8± 3.73 | 33.9± 4.95 | 34.9± 4.42 | 0.07 |
| **Booking BMI (kg/m$^2$)**[2] | 29.3 (22.4, 36.9) | 25.5 (20.8, 40.5) | 29.0 (26.5, 36.6) | 33.4 (30.0, 35.2) [a] | 0.78 |
| **Ethnicity**[3] | | | | | 0.42 |
| White | 7 (87.5) | 6 (75.0) | 4 (36.4) | 5 (62.5) | |
| Black | 0 (0.0) | 1 (12.5) | 1 (9.0) | 0 (0.0) | |
| Asian | 1 (12.5) | 1 (12.5) | 5 (45.5) | 2 (25.0) | |
| Other | 0 (0.0) | 0 (0.0) | 1 (9.0) | 1 (12.5) | |
| **Smoking status**[3] | | | | | 0.14 |
| QDP | 1 (12.5) | 0 (0.0) | 0 (0.0) | 0 (0.0) | |
| Non-smoker | 6 (75.0) | 8 (100.0) | 11 (100.0) | 8 (100.0) | |
| Smoker | 1 (12.5) | 0 (0.0) | 0 (0.0) | 0 (0.0) | |
| **Gestational age (days)**[2] | 272.5 (271.0, 276.8) | 269.5 (266.5, 274.0) | 268.0 (266.0, 270.0) | 271.5 (267.5, 274.0) [b] | 0.09 |
| **Parity**[3] | | | | | 0.55 |
| 0 | 1 (12.5) | 2 (25.0) | 1 (9.0) | 1 (12.5) | |
| 1 | 3 (37.5) | 3 (37.5) | 4 (36.4) | 4 (50.0) | |
| 2 | 2 (25.0) | 3 (37.5) | 3 (27.3) | 0 (0.0) | |
| 3 | 2 (25.0) | 0 (0.0) | 3 (27.3) | 1 (12.5) | |
| ≥4 | 0 (0.0) | 0 (0.0) | 0 (0.0) | 2 (25.0) | |
| **Mode of delivery**[3] | | | | | 0.13 |
| SVD | 1 (12.5) | 2 (25.0) | 4 (36.4) | 0 (0.0) | |
| VD-ind | 0 (0.0) | 0 (0.0) | 2 (18.2) | 0 (0.0) | |
| CS-el | 6 (75.0) | 6 (75.0) | 4 (36.4) | 4 (50.0) | |
| CS-em | 0 (0.0) | 0 (0.0) | 1 (9.0) | 2 (25.0) | |
| Unknown | 1 (12.5) | 0 (0.0) | 0 (0.0) | 2 (25.0) | |
| **Placental weight (g)**[1] | 533.3 ± 84.51 [a] | 700.0 ± 121.6 | 556.1 ± 134.4 | 838.7 ± 305.9 [a] | **0.01**[c] |
| **Birthweight (g)** [1] | 3372 ± 175.7 | 4103 ± 359.4 | 3333 ± 302.9 | 4359 ± 349.1 | **<0.001**[d] |
| **Fetal sex**[3] | | | | | 0.47 |
| Male | 5 (62.5) | 3 (37.5) | 5 (45.4) | 3 (37.5) | |
| Female | 3 (37.5) | 5 (62.5) | 6 (54.6) | 3 (37.5) | |
| Unknown | 0 (0.0) | 0 (0.0) | 0 (0.0) | 2 (25.0) | |
| **Fetal: placental weight ratio**[2] | 6.1 (5.6, 7.1)[a] | 6.1 (5.1, 6.5) | 6.1 (5.4, 7.1) | 5.1 (4.6, 5.3)[a] | 0.19 |
| **Fetal percentile**[2] | 47.30 (35.30, 58.48) | 94.45 (91.23, 97.50) | 43.90 (38.90, 83.20) | 97.50 (96.08, 97.50) [b] | **<0.001** [e] |

[1]mean ± standard deviation, [2]median (q1, q3), [3]frequency (%), [a]n=7, [b]n=6, QDP; quite during pregnancy, SVD; spontaneous vaginal delivery, VD-ind; induced vaginal delivery, CS-el; elective caesarean section, CS-em; emergency caesarean section. Bold indicates statistical significance at the 0.05

level, adjusted p-value <0.05*, ≤0.01 **, ≤0.001***, [c](GDM/AGA vs. GDM/LGA**), [d](non-GDM/AGA vs. non-GDM/LGA***, GDM/AGA vs. GDM/LGA***) [e](non-GDM/AGA vs. non-GDM/LGA**, GDM/AGA vs. GDM/LGA**).

**Supplementary Table 2: Demographics of placental samples with/without GDM and pathological fetal growth used for the immunohistochemistry experiments.**

| | Non-GDM AGA (n=9) | Non-GDM LGA (n=8) | GDM AGA (n=6) | GDM LGA (n=6) | p-value |
|---|---|---|---|---|---|
| **Maternal age (years)[1]** | 30.7 ± 5.74 | 33.6 ± 4.72 | 29.0 ± 6.57 | 30.7 ± 7.55 | 0.55 |
| **Booking BMI (kg/m$^2$) [1]** | 30.4 ± 4.35 | 24.1± 2.9 | 32.5 ± 3.4 | 33 ± 4.54 [a] | **0.001** [c] |
| **Ethnicity[2]** | | | | | 0.29 |
| White | 8 (88.9) | 6 (75.0) | 3 (50.0) | 3 (50.0) | |
| Black | 0 (0.0) | 0 (0.0) | 1 (16.7) | 0 (0.0) | |
| Asian | 1 (11.1) | 0 (0.0) | 1 (16.7) | 2 (33.3) | |
| Other | 0 (0.0) | 2 (25.0) | 1 (16.7) | 1 (16.7) | |
| **Smoking status[2]** | | | | | 0.46 |
| Ex-smoker | | | | | |
| Non-smoker | 3 (33.3) | 1 (12.5) | 0 (0.0) | 0 (0.0) | |
| Smoker | 4 (44.4) | 7 (87.5) | 5 (83.3) | 4 (66.7) | |
| Unknown | 1 (11.1) | 0 (0.0) | 0 (0.0) | 1 (16.7) | |
| | 1 (11.1) | 0 (0.0) | 1 (16.7) | 1 (16.7) | |
| **Gestational age (days)[3]** | 274 (273, 277) | 276 (273, 285.8) | 273.5 (270, 276.5) | 274.5 (270.3, 277) | 0.70 |
| **Parity[2]** | | | | | 0.42 |
| 0 | 1 (11.1) | 3 (37.5) | 3 (50.0) | 2 (33.3) | |
| 1 | 2 (22.2) | 4 (50.0) | 2 (33.3) | 4 (66.7) | |
| 2 | 4 (44.4) | 1 (12.5) | 1 (16.7) | 0 (0.0) | |
| 3 | 1 (11.1) | 0 (0.0) | 0 (0.0) | 0 (0.0) | |
| ≥4 | 1 (11.1) | 0 (0.0) | 0 (0.0) | 0 (0.0) | |
| **Mode of delivery[2]** | | | | | 0.32 |
| NVD | | | | | |
| CS-el | 0 (0.0) | 0 (0.0) | 1 (16.7) | 1 (16.7) | |
| | 9 (100.0) | 8 (100.0) | 5 (83.3) | 5 (83.3) | |
| **Placental weight (g)[1]** | 544 ± 142[d] | 642 ± 159 | 661 ± 180 | 856 ± 266 | 0.05 |
| **Birthweight (g) [1]** | 3455 ± 369 | 4238 ± 361 | 3563 ± 340 | 4118 ± 259 | **<0.001**[e] |
| **Fetal sex[3]** | | | | | 0.34 |
| Male | 7 (77.8) | 4 (50.0) | 2 (33.3) | 4 (66.7) | |
| Female | 2 (22.2) | 4 (50.0) | 4 (66.7) | 2 (33.3) | |
| **Fetal: placental weight ratio[1]** | 6.8 ± 1.7[d] | 6.9 ± 1.3 | 5.8 ± 2.1 | 5.2 ± 1.6 | 0.21 |
| **Fetal percentile[3]** | 55.2 (21.4, 75.9) | 96.9 (91.1, 97.5) | 62.8 (38.6, 86.2) | 94.7 (91.1, 97.5) | **<0.001**[f] |

[1]mean ± standard deviation, [2]frequency (%), [3]median (q1, q2), [a]n=4, [b]n=2. [c](non-GDM/AGA vs. non-GDM/LGA** & non-GDM/LGA vs GDM/LGA**), NVD; normal vaginal delivery, CS-el; elective caesarean section, [d]n=7, [e](non-GDM/AGA vs. non-GDM/LGA*** & GDM/AGA vs. GDM/LGA*), [f](non-GDM/AGA vs. non-GDM/LGA** & GDM/AGA vs. GDM/LGA*). Bold indicates statistical significance at the 0.05 level, adjusted p-value <0.05*, ≤0.01 **, ≤0.001***.

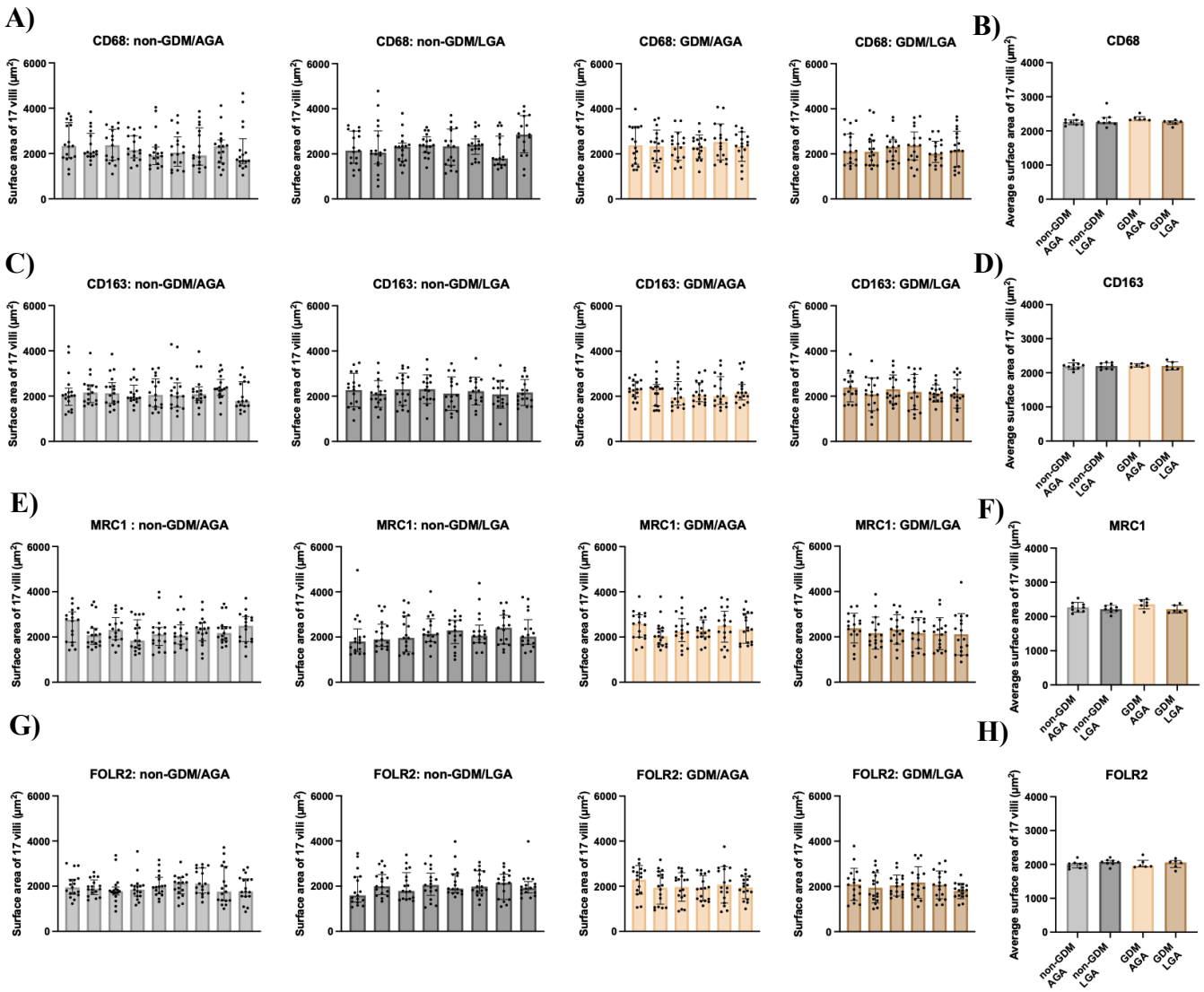


**Supplementary Figure 2: Comparable villous surface areas between participants in the non-GDM and GDM groups with AGA and LGA offspring, and among the four study groups.**

*(**A-H**) The selected surface area of 17 villi per sample was comparable across samples within the same group and between the average values for each participant across the four groups. (**A**) For CD68 analysis, data are presented as median with interquartile range and analysed by Kruskal-Wallis with Dunn's post hoc test (non-GDM/AGA; p=0.82, non-GDM/LGA; p=0.23, GDM/LGA; p=0.98) or mean with SD and analysed by one-way ANOVA with Tukey post hoc test (GDM/AGA; p= 0.95). (**B**) Analysis of the average surface area of 17 villi per sample between groups was performed using Kruskal-Wallis with Dunn's post hoc test and data are presented as median with interquartile range (p=0.12). (**C**) For CD163 analysis, data are presented as median with interquartile range and analysed by Kruskal-Wallis with Dunn's post hoc test (non-GDM/AGA; p=0.78, GDM/AGA; p=0.94) or mean with SD and analysed by one-way ANOVA with Tukey post hoc test (non-GDM/LGA; p=0.93, GDM/LGA; p= 0.71). (**D**) Analysis of the average surface area of 17 villi per sample between groups was performed using one-way ANOVA with Tukey post hoc test and data are presented as mean with SD (p=0.97). (**E**) For MRC1 analysis, data are presented as median with interquartile range and analysed by Kruskal-Wallis with Dunn's post hoc test (non-GDM/AGA; p=0.58, non-GDM/LGA; p=0.63, GDM/AGA; p=0.55) or mean with SD and analysed by one-way ANOVA with Tukey post hoc test (GDM/LGA; p=0.84). (**F**) Analysis of the average surface area of 17 villi per sample between groups was performed using one-way ANOVA with Tukey post hoc test and data are presented as mean with SD (p=0.17). (**G**) For FOLR2 analysis, data are presented as median with interquartile range and analysed by Kruskal-Wallis with Dunn's post hoc test (non-GDM/AGA; p=0.75, non-GDM/LGA; p=0.74), mean with SD and analysed by one-way ANOVA with Tukey post hoc test (GDM/AGA; p=0.55), or mean with SD and analysed by*

*Brown-Forsythe and Welch ANOVA test with Dunnett T3 post hoc test (GDM/LGA; p=0.10). (**H**) Analysis of the average surface area of 17 villi per sample between groups was performed using Kruskal-Wallis with Dunn's post hoc test and data are presented as median with interquartile range (p=0.33). Each bar represents a different sample and dots represent surface area of villi (μm$^2$). Non-GDM/AGA (n=9), non-GDM/LGA (n=8), GDM/AGA (n=6), and GDM/LGA (n=6).*

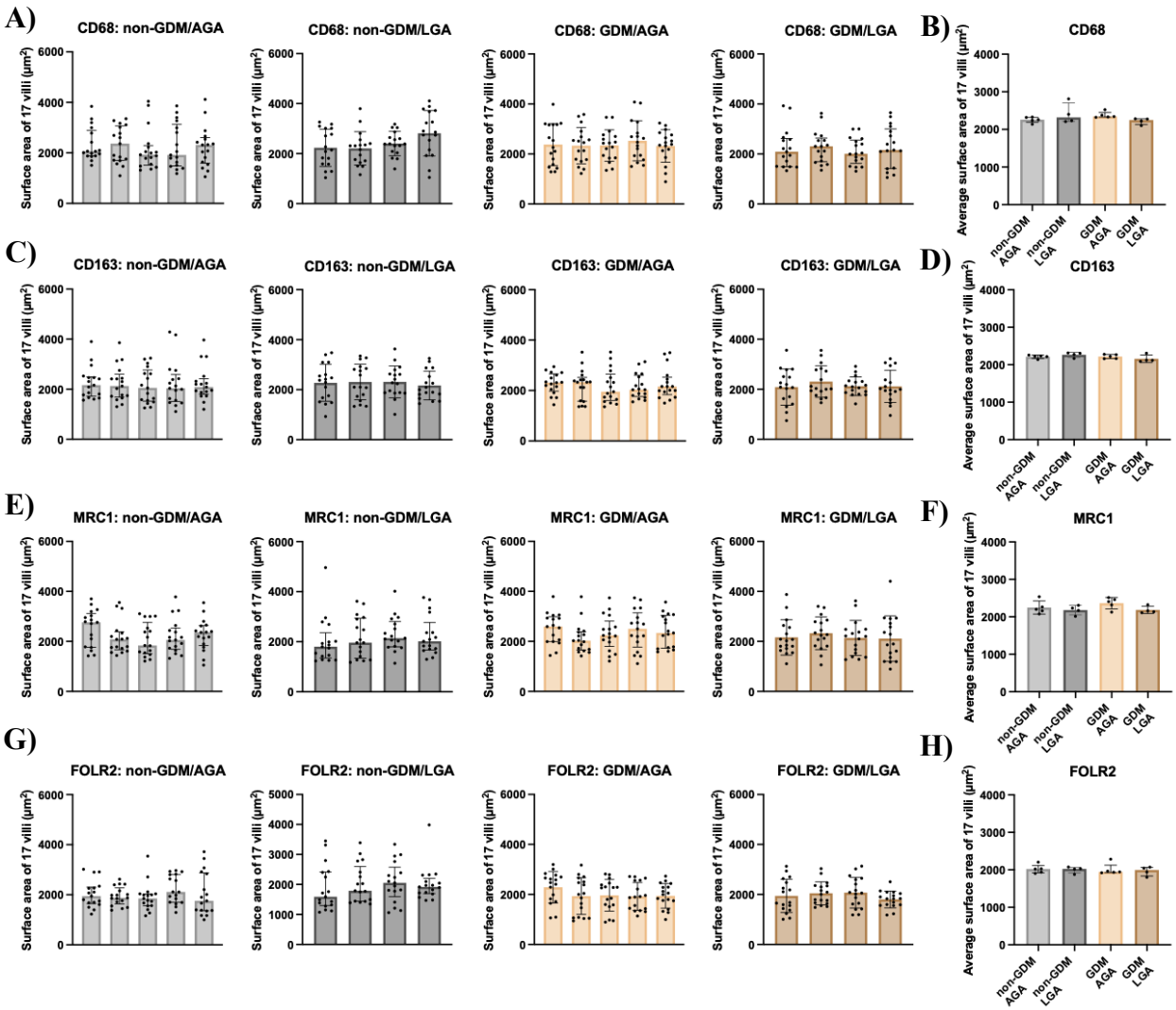


**Supplementary Figure 3: Comparable villous surface areas between participants in the non-GDM and GDM groups with AGA and LGA offspring, and among the four study groups in the smaller cohort.**

*(**A-H**) The selected surface area of 17 villi per sample was comparable across samples within the same group and between the average values for each participant across the four groups. (**A**) For CD68 analysis, data are presented as median with interquartile range and analysed by Kruskal-Wallis with Dunn's post hoc test (non-GDM/AGA; p=0.82, GDM/LGA; p=0.90) or mean with SD and analysed by one-way ANOVA with Tukey post hoc test (non-GDM/LGA; p=0.06, GDM/AGA; p= 0.92). (**B**) Analysis of the average surface area of 17 villi per sample between groups was performed using Kruskal-Wallis with Dunn's post hoc test and data are presented as median with interquartile range (p=0.07). (**C**) For CD163 analysis, data are presented as median with interquartile range and analysed by Kruskal-Wallis with Dunn's post hoc test (non-GDM/AGA; p=0.95, GDM/AGA; p=0.87) or mean with SD and analysed by one-way ANOVA with Tukey post hoc test (non-GDM/LGA; p=0.91, GDM/LGA; p= 0.71). (**D**) Analysis of the average surface area of 17 villi per sample between groups was performed using one-way ANOVA with Tukey post hoc test and data are presented as mean with SD (p=0.22). (**E**) For MRC1 analysis, data are presented as median with interquartile range and analysed by Kruskal-Wallis with Dunn's post hoc test (non-GDM/AGA; p=0.39, non-GDM/LGA; p=0.31, GDM/LGA; p=0.84) or mean with SD and analysed by one-way ANOVA with Tukey post hoc test (GDM/AGA; p=0.44). (**F**) Analysis of the average surface area of 17 villi per sample between groups was performed using one-way ANOVA with Tukey post hoc test and data are presented as mean with SD (p=0.22). (**G**) For FOLR2 analysis, data are presented as median with interquartile range and analysed by Kruskal-Wallis with Dunn's post hoc test (non-GDM/AGA; p=0.58, non-GDM/LGA; p=0.57), mean with SD and analysed by one-way ANOVA with Tukey post hoc test (GDM/AGA; p=0.37), or mean with SD and analysed by Brown-Forsythe and Welch ANOVA test with Dunnett T3 post hoc test (GDM/LGA; p=0.45). (**H**) Analysis*

795 *of the average surface area of 17 villi per sample between groups was performed using Kruskal-Wallis*
796 *with Dunn's post hoc test and data are presented as median with interquartile range (p=0.98). Each bar*
797 *represents a different sample and dots represent surface area of villi ($\mu m^2$).*

**Supplementary Table 3: Demographics of a subgroup of placental samples with/without GDM categorised by fetal sex in the RT-qPCR experiments.**

| | Non-GDM Female (n=6) | Non-GDM Male (n=6) | GDM Female (n=6) | GDM Male (n=6) | p-value |
|---|---|---|---|---|---|
| **Maternal age (years)[1]** | 31.50± 6.442 | 28.50± 4.231 | 31.67± 5.465 | 31.33± 2.422 | 0.64 |
| **Booking BMI ($kg/m^2$)[2]** | 34.17 (22.8, 37.4) | 24.53 (21.5, 31.6) | 32.80 (27.7, 39.1) | 27.25 (23.0, 31.3) | 0.38 |
| **Ethnicity[3]** | | | | | 0.76 |
| White | 3 (50.0) | 4 (66.7) | 3 (50.0) | 2 (33.3) | |
| Black | 1 (16.7) | 0 (0.0) | 0 (0.0) | 0 (0.0) | |
| Asian | 2 (33.3) | 2 (33.3) | 2 (33.3) | 4 (66.7) | |
| Other | 0 (0.0) | 0 (0.0) | 1 (16.7) | 0 (0.0) | |
| **Smoking status[3]** | | | | | 0.37 |
| QDP | 1 (16.7) | 0 (0.0) | 0 (0.0) | 0 (0.0) | |
| Non-smoker | 5 (83.3) | 6 (100) | 6 (100.0) | 6 (100.0) | |
| **Gestational age (days)[2]** | 272.5 (269.5, 280.8) | 269.5 (267.5, 278.8) | 269.5 (266.0, 281.0) | 268.5 (266.8, 275.8) | 0.86 |
| **Parity[3]** | | | | | 0.86 |
| 0 | 1 (16.7) | 3 (50.0) | 2 (33.3) | 1 (16.7) | |
| 1 | 1 (16.7) | 1 (16.7) | 2 (33.3) | 3 (50.0) | |
| 2 | 2 (33.3) | 2 (33.3) | 1 (16.7) | 1 (16.7) | |
| 3 | 2 (33.3) | 0 (0.0) | 1 (16.7) | 1 (16.7) | |
| **Mode of delivery[3]** | | | | | 0.60 |
| SVD | 2 (33.3) | 2 (33.3) | 2 (33.3) | 2 (33.3) | |
| VD-ind | 0 (0.0) | 0 (0.0) | 1 (16.7) | 1 (16.7) | |
| CS-el | 4 (66.7) | 4 (66.7) | 2 (33.3) | 1 (16.7) | |
| CS-em | 0 (0.0) | 0 (0.0) | 1 (16.7) | 2 (33.3) | |
| **Placental weight (g)[1]** | 508.8± 68.91 | 679.2± 168.7 | 607.1± 130.6 | 731.8 ± 231.7 | 0.12 |
| **Birthweight (g) [1]** | 3425 ± 268.0 | 4073 ± 473.6 | 3454 ± 394.2 | 3879 ± 709.6 | 0.08 |
| **Fetal: placental weight ratio[2]** | 6.6 (6.1, 7.4) | 6.2 (4.9, 7.8) | 5.7 (5.0, 6.5) | 5.2 (4.6, 6.5) | 0.15 |
| **Fetal percentile[2]** | 47.5 (23.0, 70.2) | 93.5 (86.2, 96.2) | 54.3 (39.5, 81.2) | 91.0 (57.0, 94.8) | 0.11 |

[1]mean ± standard deviation, [2]median (q1, q3), [3]frequency (%), QDP; quite during pregnancy, SVD; spontaneous vaginal delivery, VD-ind; induced vaginal delivery, CS-el; elective caesarean section, CS-em; emergency caesarean section. Statistical significance at the 0.05 level.

**Supplementary Table 4: Demographics of a subgroup of placental samples with/without GDM categorised by fetal sex in the immunohistochemistry experiments.**

| | Non-GDM Female (n=4) | Non-GDM Male (n=4) | GDM Female (n=4) | GDM Male (n=4) | p-value |
|---|---|---|---|---|---|
| **Maternal age (years)[1]** | 35.3 ± 4.57 | 32.3 ± 3.10 | 26.8 ± 5.62 | 32.0 ± 8.45 | 0.27 |
| **Booking BMI (kg/m$^2$)[1]** | 26.1 ± 3.14 | 26.4 ± 3.83 | 31.0 ± 2.96 | 32.4 ± 3.89 | 0.05 |
| **Ethnicity[2]** | | | | | 0.11 |
| White | 3 (75.0) | 4 (100.0) | 2 (50.0) | 1 (25.0) | |
| Black | 0 (0.0) | 0 (0.0) | 1 (25.0) | 0 (0.0) | |
| Asian | 0 (0.0) | 0 (0.0) | 0 (0.0) | 3 (75.0) | |
| Other | 1 (25.0) | 0 (0.0) | 1 (25.0) | 1 (25.0) | |
| **Smoking status[2]** | | | | | 0.60 |
| Non-smoker | 2 (50.0) | 3 (75.0) | 3 (75.0) | 3 (75.0) | |
| Ex-smoker | 2 (50.0) | 0 (0.0) | 0 (0.0) | 1 (25.0) | |
| Smoker | 0 (0.0) | 1 (25.0) | 0 (0.0) | 0 (0.0) | |
| Unknown | 0 (0.0) | 0 (0.0) | 1 (25.0) | 0 (0.0) | |
| **Gestational age (days)[3]** | 274.5 (273.3, 286.3) | 273.0 (266.3, 285.8) | 274.0 (271.5, 279.5) | 274.0 (268.8, 276.3) | 0.91 |
| **Parity[3]** | | | | | 0.32 |
| 0 | 2 (50.0) | 0 (0.0) | 3 (75.0) | 0 (0.0) | |
| 1 | 1 (25.0) | 2 (50.0) | 1 (25.0) | 3 (75.0) | |
| 2 | 1 (25.0) | 1 (25.0) | 0 (0.0) | 1 (25.0) | |
| 3 | 0 (0.0) | 0 (0.0) | 0 (0.0) | 0 (0.0) | |
| ≥4 | 0 (0.0) | 1 (25.0) | 0 (0.0) | 0 (0.0) | |
| **Mode of delivery[2]** | | | | | >0.99 |
| NVD | 0 (0.0) | 0 (0.0) | 1 (25.0) | 0 (0.0) | |
| CS-el | 4 (100.0) | 4 (100.0) | 3 (75.0) | 4 (100.0) | |
| **Placental weight (g)[1]** | 531 ± 151 | 589 ± 112 | 620 ± 212 | 758 ± 211 | 0.35 |
| **Birthweight (g) [1]** | 4119 ± 510 | 3838 ± 697 | 3725 ± 278 | 3795 ± 455 | 0.71 |
| **Fetal: placental weight ratio[3]** | 7.7 (6.7, 9.9) | 6.35 (6.0, 7.2) | 6.1 (4.8, 8.9) | 4.6 (4.3, 7.0) | 0.15 |
| **Fetal percentile[3]** | 94.5 (77.0, 97.5) | 90.6 (38.3, 95.9) | 84.3 (52.6, 87.9) | 91.1 (50.2, 91.6) | 0.33 |

[1]mean ± standard deviation, [2]frequency (%), [3]median (q1, q3), SVD; spontaneous vaginal delivery, CS-el; elective caesarean section. Statistical significance at the 0.05 level.

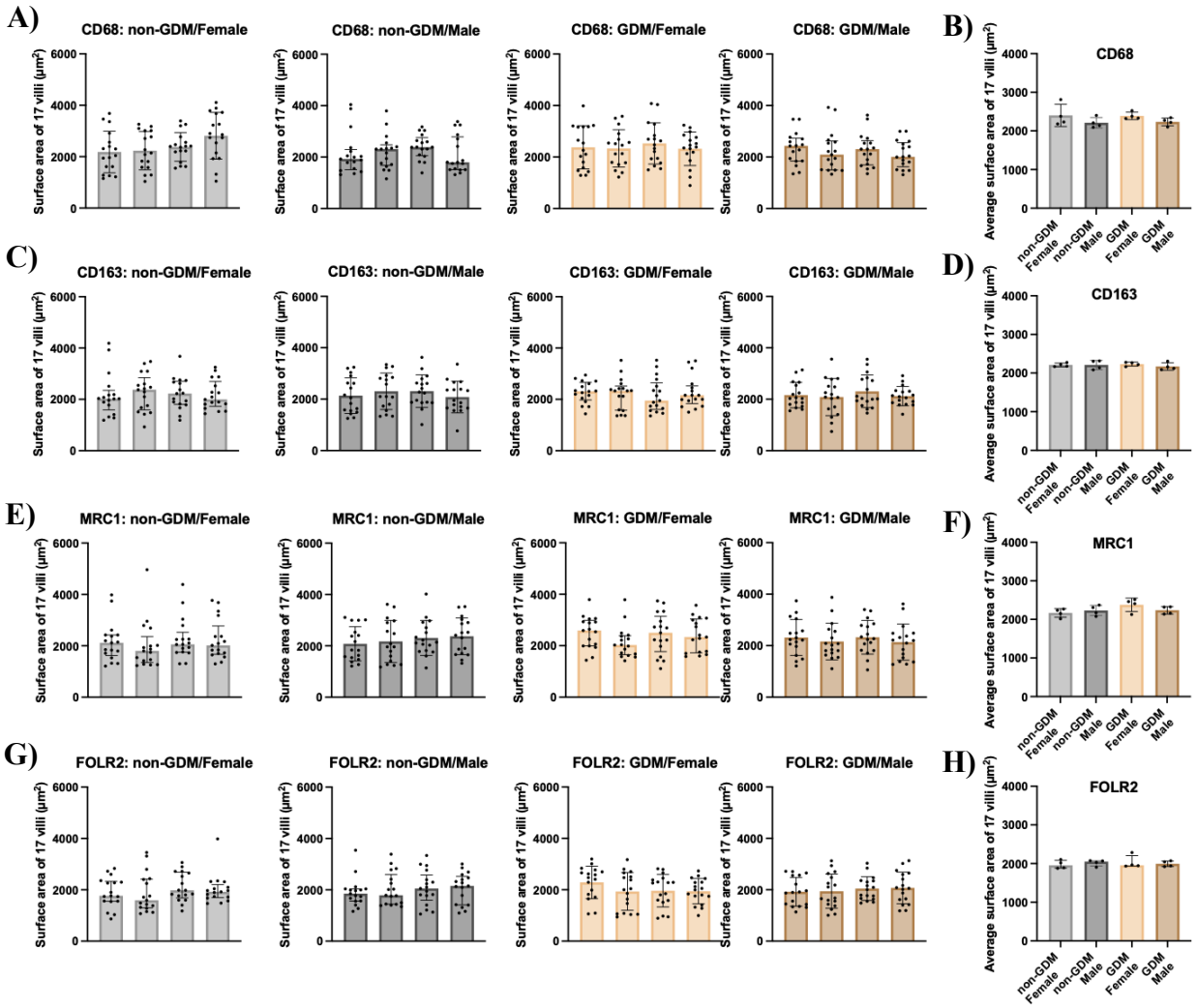


**Supplementary Figure 4: Comparable villous surface areas between participants in the non-GDM and GDM groups with female and male offspring, and among the four study groups.**

*(**A-H**) The selected surface area of 17 villi per sample was comparable across samples within the same group and between the average values for each participant across the four groups. (**A**) For CD68 analysis, data are presented as median with interquartile range and analysed by Kruskal-Wallis with Dunn's post hoc test (non-GDM/Male; p=0.21, GDM/Male; p=0.75) or mean with SD and analysed by one-way ANOVA with Tukey post hoc test (non-GDM/Female; p=0.08, GDM/Female; p= 0.26). (**B**) Analysis of the average surface area of 17 villi per sample between groups was performed using one-way ANOVA with Tukey post hoc test and data are presented as mean with SD (p=0.31). (**C**) For CD163 analysis, data are presented as median with interquartile range and analysed by Kruskal-Wallis with Dunn's post hoc test (non-GDM/Female; p=0.86, GDM/Female; p=0.84) or mean with SD and analysed by one-way ANOVA with Tukey post hoc test (non-GDM/Male; p=0.66, GDM/Male; p= 0.69). (**D**) Analysis of the average surface area of 17 villi per sample between groups was performed using one-way ANOVA with Tukey post hoc test and data are presented as mean with SD (p=0.77). (**E**) For MRC1 analysis, data are presented as median with interquartile range and analysed by Kruskal-Wallis with Dunn's post hoc test (non-GDM/Female; p=0.45, GDM/Female; p=0.31) or mean with SD and analysed by one-way ANOVA with Tukey post hoc test (non-GDM/Male; p=0.64, GDM/Male; p= 0.79). (**F**) Analysis of the average surface area of 17 villi per sample between groups was performed using one-way ANOVA with Tukey post hoc test and data are presented as mean with SD (p=0.20). (**G**) For FOLR2*

*analysis, data are presented as median with interquartile range and analysed by Kruskal-Wallis with Dunn's post hoc test (non-GDM/Female; p=0.39, non-GDM/Male; p=0.67), or mean with SD and analysed by one-way ANOVA with Tukey post hoc test (GDM/Female; p=0.30, GDM/Male; p=0.84). (**H**) Analysis of the average surface area of 17 villi per sample between groups was performed using Kruskal-Wallis with Dunn's post hoc test and data are presented as median with interquartile range (p=0.86). (**A**,**C,E,G**) Each bar represents a different sample and dots represent surface area of villi ($\mu m^2$). Non-GDM/Female (n=4), non-GDM/Male (n=4), GDM/Female (n=4), and GDM/Male (n=4).*